URS 708-4

INTERACTION OF FALLOUT WITH FIRES

Final Report

September 1969

by

Peter O. Strom
Carl F. Miller
URS RESEARCH COMPANY
155 Bovet Road
San Mateo, California 94402

for

OFFICE OF CIVIL DEFENSE
Office of the Secretary of the Army
Department of the Army
Washington, D.C. 20310

Contract No. DAHC20-70-C-0214
OCD Work Units 3124B and 3124C

OCD REVIEW NOTICE

This report has been reviewed in the Office of Civil Defense and approved for publication. Approval does not signify that the contents necessarily reflect the views and policies of the Office of Civil Defense.

URS 708-4
SUMMARY

INTERACTION OF FALLOUT WITH FIRES

by

Peter O. Strom
Carl F. Miller
URS RESEARCH COMPANY
155 Bovet Road
San Mateo, California 94402

September 1969

Office of Civil Defense
Office of the Secretary of the Army
Department of the Army
Washington, D.C. 20310

OCD Contract No. DAHC20-70-C-0214
OCD Work Units 3124B and 3124C

SUMMARY

THE ~~This~~ report provides parametric relationships describing the possible interactions of fallout particles with air and gas currents arising from fires of circular area and from line fires. The effects that result from fallout – fire interactions due to varying fire dimensions and intensities, ambient wind velocities, fallout particle sizes, height of particle – fire plume interaction and other variables are given. Fallout field dislocations caused by fires are estimated for a number of fallout, fire, and ambient wind conditions relative to fields postulated to exist in the absence of fires. Under a number of fire input, meteorological, and fallout parameter values, the model output suggest that considerable alterations in fallout patterns could be produced.

TABLE OF CONTENTS

LIST OF ILLUSTRATIONS

LIST OF TABLES

INTRODUCTION

Were nuclear warfare to occur, it is generally to be expected that most nuclear detonations near populated areas would generate fires. Since postulated nuclear attack situations often refer to a timed sequence of detonations, each of which could affect a specific area, fires may be in a number of stages of development and intensity at a time when fallout might approach an area affected by fire. It is evident that the local effects of fires on air movement can influence the trajectories of particles which are transported toward the burning region. Estimation of the extent to which fallout deposition might be altered spatially and temporally by the presence of fires relative to that for a fire-free area has been the subject of the present study.

In the investigation of the effects that fires may have on the fallout environment and on the motion of the particles themselves, a number of factors have not been considered. For example, the temperatures to which particles might be subjected in a fire have not been studied since it would generally be low relative to temperatures to which most particles within the nuclear fireball or cloud would have been previously exposed. Thermochemical effects upon low-melting fission product depositions have been likewise ignored. From the view of fire – fallout interaction, only parameters pertaining to the effects of ambient and fire-generated air velocities on the transport of fallout particles were considered in the study.

BACKGROUND

In the theoretical examination of fire regimes and buoyant plumes, the literature is richest in studies in which buoyant plumes perturbing motionless media subject to a variety of mathematical constraints are examined. Among the first to examine this subject was Schmidt[1] in studies of convective air plumes in an incompressible, uniform atmosphere. Among other contributors to the understanding of convection columns above circular or point-source fires are Sutton,[2] Rouse, Yih and Humphreys,[3] Broido and McMasters,[4] Priestly and Ball,[5] Morton, Taylor and Turner,[6] Murgai and Emmons,[7] Morton,[8] and Nielsen, Tao and Wolf.[9] Depending upon the relationships that an author has chosen to define the problem, mathematical solutions have been derived for convection column problems in closed form or as a series of numerical solutions from machine computations. Each approach suffers from the assumptions that the author has been required to make concerning the physical nature of a mass fire or a convective plume because of the lack of a sufficient source of quantitative experimental or observational input data.

In the present study of the effects of fire on fallout, the authors have chosen to adapt the results of Nielsen, Tao, and Wolf[9] for use in representing convection columns. The approach of Nielsen, et al., leads to numerical solutions which describe the behavior of a number of column parameters (column radius, vertical velocity, temperature, weight fraction of gaseous fuel) as a function of distance above the ground surface. As with other modeling studies of convection columns, the consequences of several assumptions are present in these numerical solutions. The principal assumptions are (1) a plume boundary exists beyond which ambient conditions are present, and (2) at any given altitude, parameters which characterize the convection column (gas density, vertical velocity, existing gas species, and enthalpy) are uniform within the boundary. Other assumptions, made explicit in the treatment, form part of the theory and allow the construction of the convection column from

the surface to relatively high altitudes. In this investigation of fire–fallout interactions, the numerical solutions of Nielsen, et al., have been approximated by functions in closed form, which allows greater facility in computation. The following relationships are, then, based closely upon the numerical solutions developed by Nielsen, et al.

PHENOMENOLOGICAL DESCRIPTION OF FIRE PLUMES

The vertical velocities existing within a convection plume all exhibit a maximum value above a uniformly burning area of circular dimension. The conditions are given for a fuel gas surface temperature of 350°F, and entrainment coefficient of 0.17, and an atmospheric lapse rate of 0.005355°F per foot. The maximum vertical velocity that exists under these conditions within the plume may be closely approximated by

$$U_0(F,R) = 1460 \left(1 - e^{-4.02 \times 10^{-4} R}\right) F^{1/5} \qquad (1)$$

where F is the fuel gas generation rate of the fire in $lb/ft^2 sec$,
R is the radius of the fire in feet at ground level,
$U_0(F,R)$ is the maximum vertical velocity in the plume in ft/sec.

As given in Equation 1, the maximum plume vertical velocity of a fire at a given gas generation rate per unit area increases toward an asymptotic value as the size of the burning area increases. Maximum velocity in the plume is quite insensitive to the gas generation rate per unit area.

The height at which the maximum velocity occurs varies with the fuel gas generation rate and the ground radius of the fire. This height is closely represented by the relation

$$Z_0(F,R) = 66,470 \left(1 - e^{-4.80 \times 10^{-5} R}\right) F^{2/5} \qquad (2)$$

in which $Z_0(F,R)$ is the altitude of the maximum velocity in feet, and F and R are as defined for Equation 1. At constant fuel gas generation rate, the height at which the maximum fire velocity occurs approaches a constant value asymptotically as the radius of the surface area afire becomes very large and, at constant radius, it increases relatively slowly with increasing fuel gas generation rate.

The vertical velocity of the gases at any height within the plume may be represented by

$$U(F,R,Z) = \frac{U_0(F,R)Z_0(F,R)}{Z} e \left(1 - \frac{Z_0(F,R)}{Z}\right) \quad (3)$$

where $U(F,R,Z)$ is vertical velocity in ft/sec,
$U_0(F,R)$ is maximum vertical velocity in ft/sec,
$Z_0(F,R)$ is the altitude of maximum velocity in feet,
Z is the height within the plume in feet,
F is fuel gas generation rate in lb/ft^2-sec, and
R is the surface radius of the fire in feet.

Under conditions of constant fuel gas generation and fire surface radius, the vertical velocity thus rapidly increases with height from a value of zero at the surface to its maximum value of $U_0(F,R)$ at $Z_0(F,R)$. At heights greater than $Z_0(F,R)$, the velocity diminishes rapidly with height, although at relatively great heights (16,000 ft) substantial vertical plume velocities may still be present when the values of R and F are large.

The magnitude of the vertical plume velocities above fires at different altitudes is, as stated earlier, essential in the treatment of the influence of fires on the transport of falling particles. In addition, the radial wind velocities generated by fires are required to describe fallout – fire interactions. In the treament of convection plumes by Nielsen, et al., wind velocities are discontinuous at the boundary of the plume such that only vertical velocities exist within the plume and horizontal winds at the boundary. At the boundary, an assumption about the relationship between the radial and vertical gas velocities is made; it is given by

$$\rho_\infty V = \alpha \rho U \quad (4)$$

where ρ_∞ is the ambient air density at the height X infinitely removed from the plume,
V is the radial velocity of air entering the plume at height Z,

α is the entrainment constant of air and is assumed to have a value of 0.17, and

U is the vertical velocity of gases within the plume at height Z.

In Equation 4, it is assumed that the air entrainment is proportional to the mass velocity of plume gases for media where density differences can be large.

To obtain the radial velocity, V, as a function of altitude, the density functions ρ_∞ and ρ are required. The relation

$$\rho = \frac{P\bar{M}}{R'T} \tag{5}$$

is sufficient to provide density estimates both within and external to the plume. In Equation 5, ρ is the density, P is the pressure, $\bar{M}$ is the average gas molecular weight, R' is the gas constant, and T is the absolute temperature. It is assumed that the pressures within and external to the plume are identical at all heights. External to the plume the pressure is given by

$$P = \frac{R'T_\infty\rho_\infty}{\bar{M}} \tag{6}$$

and the atmospheric temperature by

$$T_\infty = T_{\infty 0} - LZ \tag{7}$$

where T_∞ is the absolute ambient temperature in degrees Kelvin at height Z,

$T_{\infty 0}$ is the absolute ambient temperature at ground level, and

L is the lapse rate.

The density of ambient air with height above sea level may be represented quite accurately by the relation

$$\rho_\infty(Z) = 1.226 \times 10^{-3}\, e^{-\,3.245 \times 10^{-5} Z} \tag{8}$$

where $\rho_\infty(Z)$ is in gm/cm^3.

Substitution of Equations 7 and 8 in Equation 6 gives, for the air pressure as a function of altitude,

$$P(Z) = \frac{R'}{\bar{M}}\left(T_{\infty 0} - 2.975 \times 10^{-3} Z\right)\left(1.226 \times 10^{-3}\ e^{-3.245 \times 10^{-5} Z}\right) \qquad (9)$$

where P(Z) is in atmospheres when

R' is 82.07 cc-atm/deg,

$\bar{M}$ is average air molecular weight in grams, and

L is 2.975×10^{-3} deg K/ft

If it is assumed that the average molecular weight of the gases within the plume is the same as that of ambient air, then

$$\rho = \frac{\left(T_{\infty 0} - 2.975 \times 10^{-3} Z\right)\left(1.226 \times 10^{-3}\ e^{-3.245 \times 10^{-5} Z}\right)}{T_p(Z)} \qquad (10)$$

where $T_p(Z)$ is the plume temperature in degrees Kelvin at the height Z and a lapse rate of 2.975×10^{-3} deg K/ft is assumed. The variation of temperature within the plume, $T_p(Z)$, may be obtained through the following relations:

$$Z_0^* = 2RF^{2/5} \qquad (11)$$

for the height Z_0^* at which the temperature maximum occurs in the convection column. The temperature variation with height from the surface to the height at which the maximum occurs is given by

$$T = 1544\left[1 - e^{-4.24\left(Z/Z_0^*\right)^2}\right] + 449.7;\ Z \le Z_0^* \qquad (12)$$

and, for greater heights,

$$T = 3654\ e^{-1.342\ Z/Z_0^*} + 1072\ e^{-0.2656\ Z/Z_0^*} + 255;\ Z \ge Z_0^* \qquad (13)$$

The gas density within the plume is then related to the height (and surface fire area and gas generation rate) by the following functions:

$$\rho = \frac{\left(T_{\infty 0} - 2.975 \times 10^{-3} Z\right)\left(1.226 \times 10^{-3}\ e^{-\ 3.245 \times 10^{-5} Z}\right)}{1544\left[1 - e^{-\ 4.24\left(Z/Z_0^*\right)^2}\right] + 449.7} \quad \text{for } Z \le Z_0^* \qquad (14)$$

and

$$\rho = \frac{\left(T_{\infty 0} - 2.975 \times 10^{-3} Z\right)\left(1.226 \times 10^{-3}\ e^{-\ 3.245 \times 10^{-5} Z}\right)}{3654\ e^{-\ 1.342\left(Z/Z_0^*\right)} + 1072\ e^{-\ 0.2656\ Z/Z_0^*} + 255} \quad \text{for } Z \ge Z_0^* \qquad (15)$$

As a result the radial wind velocities may be calculated from

$$V = \frac{0.17\left(T_{\infty 0} - 2.975 \times 10^{-3} Z\right) U_0 Z_0\ e^{\left(1 - Z_0/Z\right)}}{\left\{1544\left[1 - e^{-\ 4.24\left(Z/Z_0^*\right)^2}\right] + 449.7\right\} Z} \quad \text{for } Z \le Z_0^* \qquad (16)$$

and

$$V = \frac{0.17\left(T_{\infty 0} - 2.975 \times 10^{-3} Z\right) U_0 Z_0\ e^{\left(1 - Z_0/Z\right)}}{\left\{3654\ e^{-\ 1.342\left(Z/Z_0^*\right)} + 1072\ e^{-\ 0.2656\left(Z/Z_0^*\right)} + 255\right\} Z} \quad \text{for } Z \ge Z_0^* \qquad (17)$$

In Equations 17 and 18, the radial velocity, V, is in feet per second. The radial velocity is relatively insensitive to the ambient surface temperature, $T_{\infty 0}$, within ranges which are normally encountered. The value of 280°K was chosen as $T_{\infty 0}$ for the purposes of plotting both vertical and radial velocities as functions of altitude within and at the boundary of plumes generated by sources of varying areas and gas generation rates. The results are given in Figures 1 through 4. The data plotted in the figures represent conditions

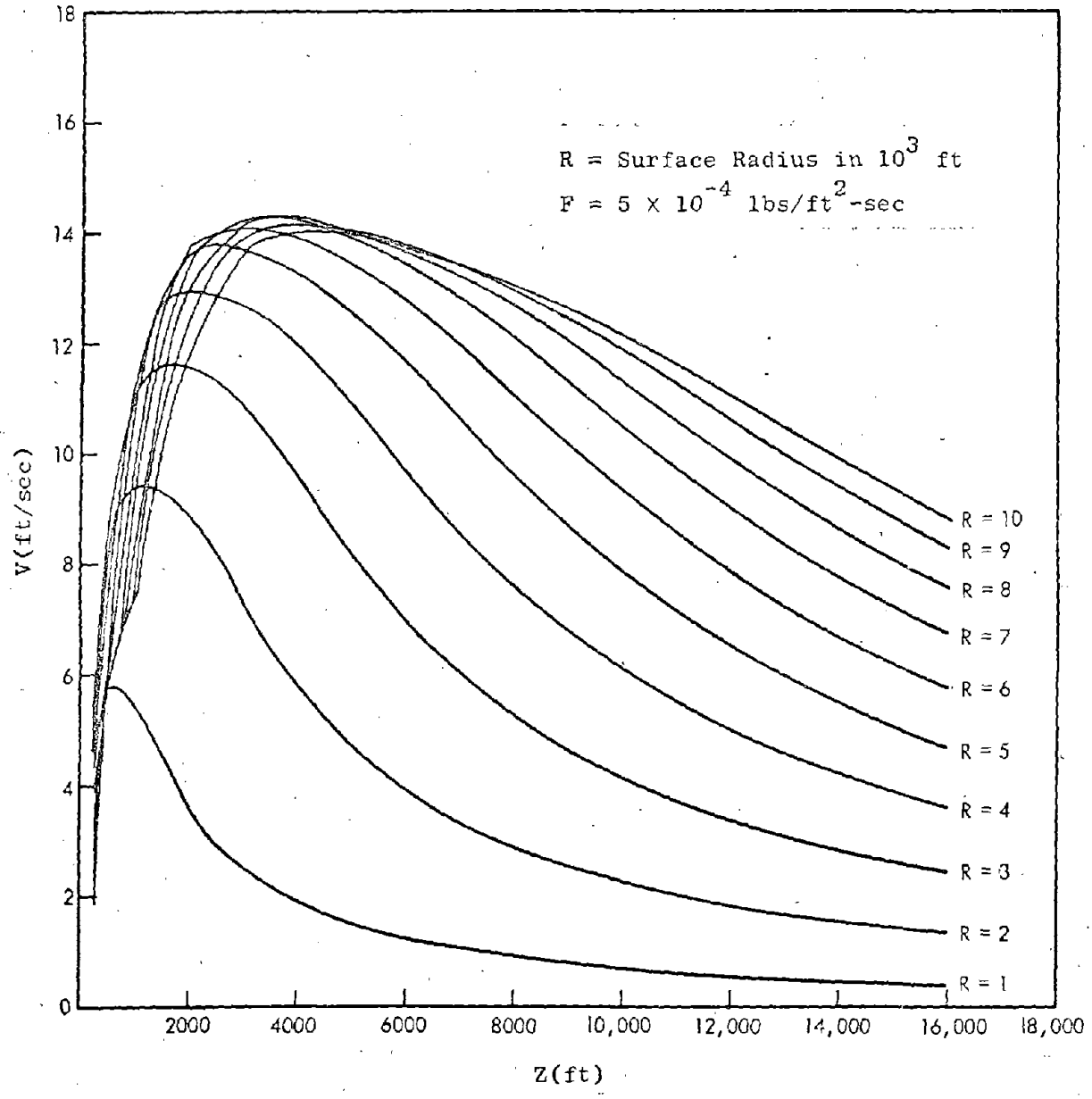

Fig. 1. Radial Velocity as a Function of Height

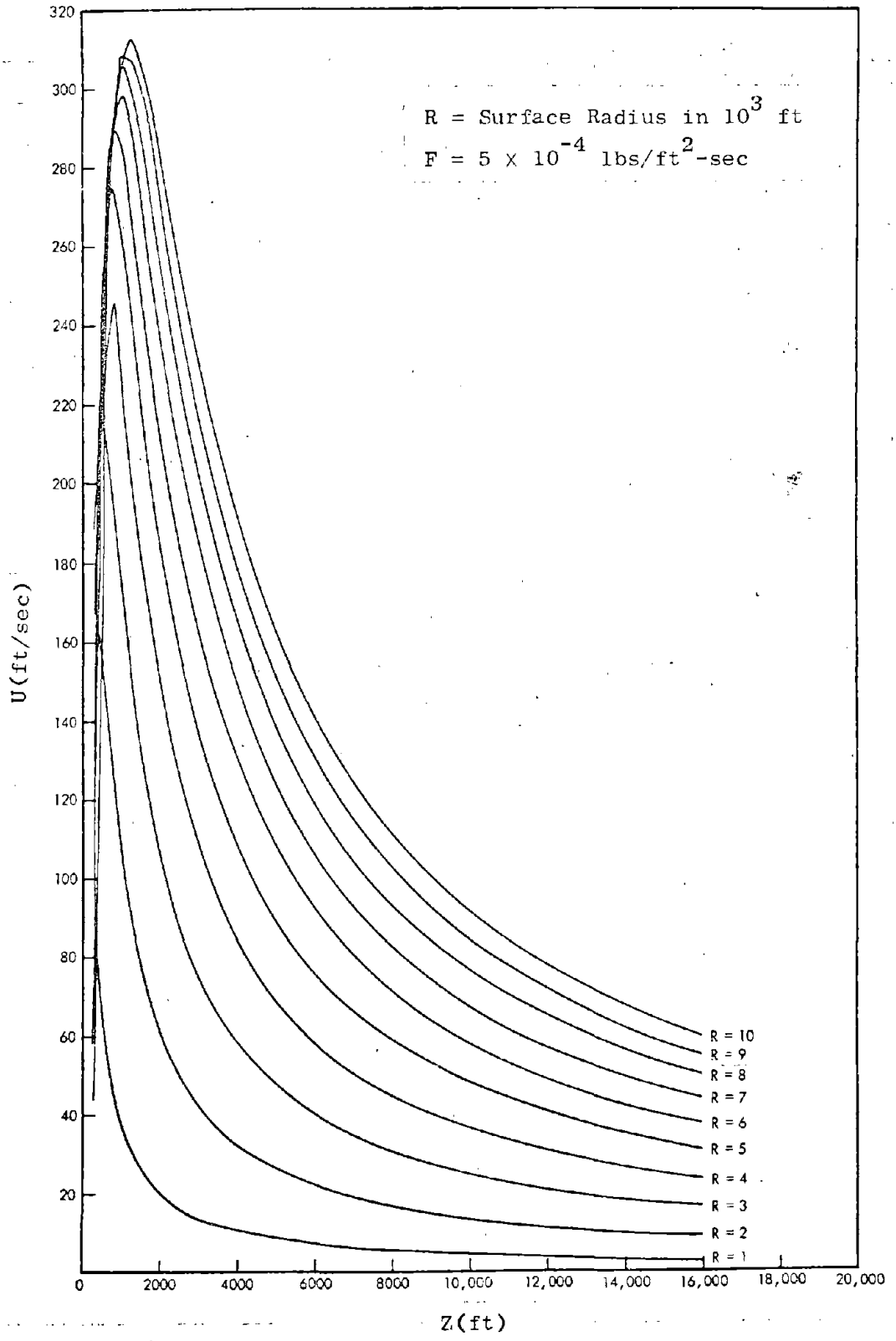

Fig. 2. Vertical Velocity as a Function of Height

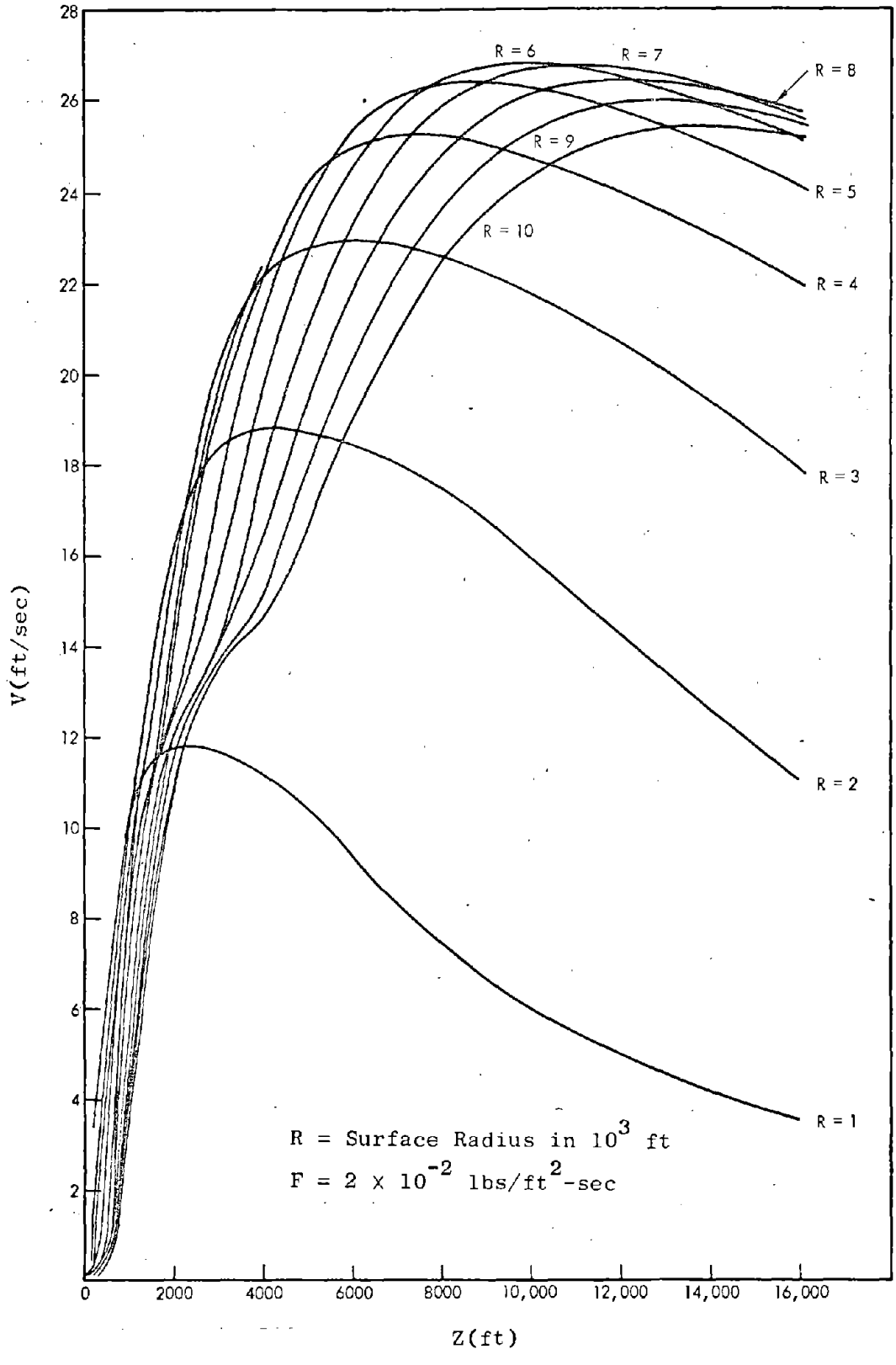

Fig. 3. Radial Velocity as a Function of Height

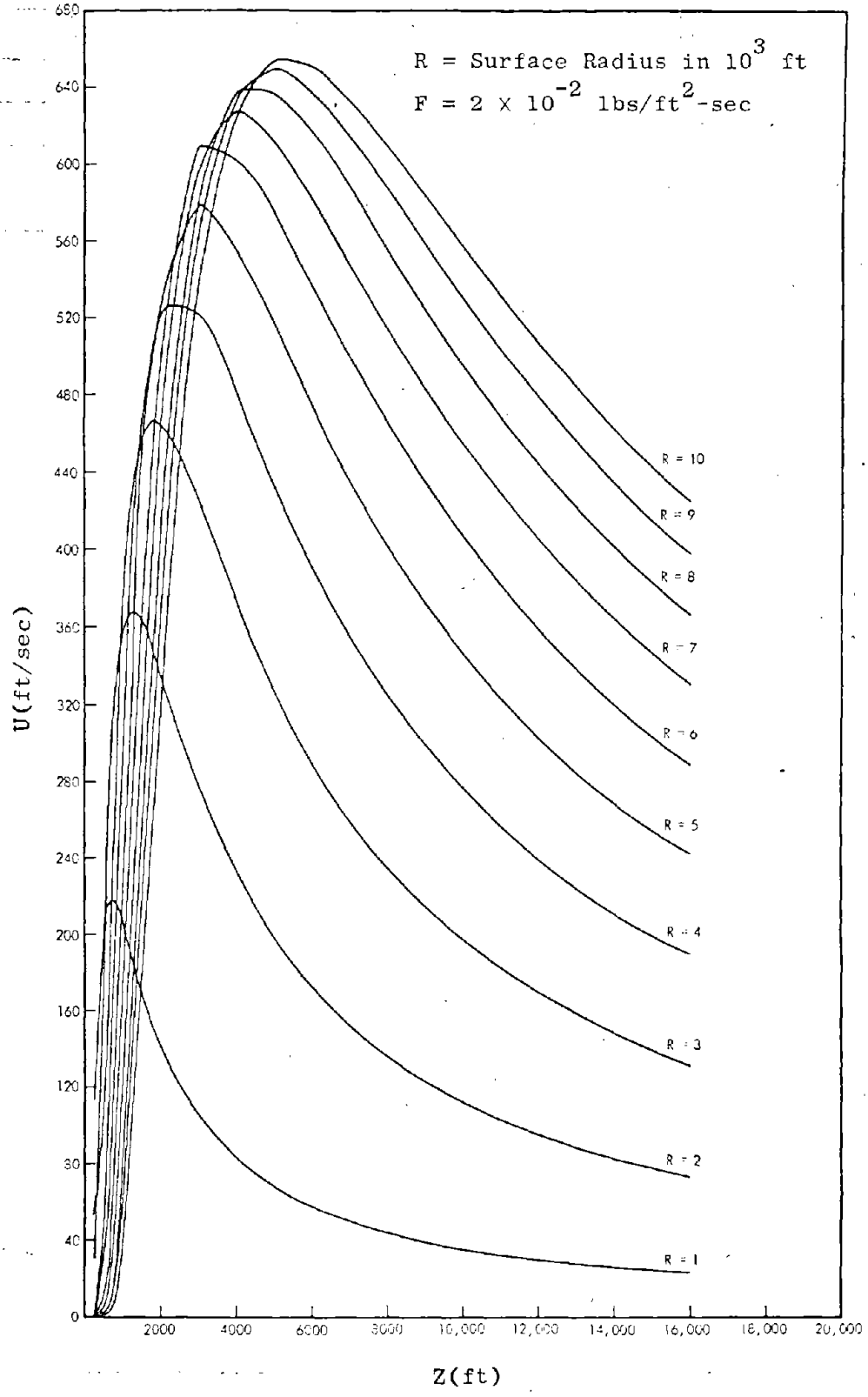

Fig. 4. Vertical Velocity as a Function of Height

that bracket what is considered to be the fuel gas generation rate associated with firestorms,[10] (i.e., 2.70×10^{-3} to 3.60×10^{-3} lbs/ft^2-sec). The vertical velocity is much greater than the radial velocity for all comparable cases, although both are of sufficient magnitude to influence particle fall rates for particles with diameters in the range commonly found in local fallout.

Maximum plume heights, for normal lapse rates, were assumed to vary in proportion to the total energy release rate raised to the one-fourth power, as reported by Morton, et al.[6] However, the experimental observations of Countryman[12] and Gaines[13] indicate the coefficient given by Morton for mass fires to be low by approximately a factor of two; with this correction applied under the circumstances of large fires of the FLAMBEAU types, Morton's relation may be represented by:

$$Z_{max} = 5520\ R^{1/2} F^{1/4} \qquad (18)$$

where Z_{max} is in feet,
R is in feet, and
F is the gas generation rate in lbs/ft^2-sec.

With regard to the interactions of fallout particles with stationary fire plumes, fire models alone do not describe observed phenomena. Observations of particle interactions with fire plumes have been reported by Broido and McMasters,[4] Countryman[11,14] and others. Broido's findings indicate that fallout deposition in the presence of a convection column can be displaced further downwind than that deposited in the absence of a fire. In addition, he found that deposition in the "shadow" of the column could be reduced from that expected under no-fire conditions. Countryman observed during FLAMBEAU studies that smoke generated in the upwind direction from a convection column (or no-lift balloons released upwind from the fire) passed about the column along paths that could be closely represented by streamline flow about a solid object. In the near lee of the fire, eddies and turbulence were observed. Were there no other interactions, the fallout – fire phenomena could be described by means of a stream function of the form:

$$\psi = U_0 y - \frac{a^2 U_0 y}{x^2 + y^2} \tag{19}$$

where U_0 is the ambient wind velocity, a is the radius of the plume, and the origin of the x - y coordinate system (i.e., the horizontal plane) is at the center of the plume. The altitude is constant. The velocity function would then be given by

$$V_x = -\frac{\partial \psi}{\partial y} = -U_0 + \frac{a^2 U_0}{r^2} - \frac{2a^2 U_0 y^2}{r^4} \tag{20}$$

and

$$V_y = \frac{\partial \psi}{\partial y} = \frac{2a^2 U_0 xy}{r^4} \tag{21}$$

where $x^2 + y^2 = r^2$.

The effect of the stream function would be to alter the velocities and path of ambient wind currents (and particles) in the localized region surrounding the plume. Behavior of this sort does occur, as evidenced by Countryman's observations. However, this behavior must be modified by the evidence of the "shadowing" which Broido obtained in his experiments. The observations are consistent with the following arguments:

1. A fire-generated convection column has air volume intake rates (varying with altitude) that are characteristic of a given set of fire parameters.

2. Inward-directed wind velocities generated by fires are of the same magnitude encountered in normally occurring ambient winds.

3. On the basis of items 1 and 2 and the observations noted, it is assumed that air volumes (and their associated fallout particles) characteristic of convection column requirements will be accepted from ambient winds. The remaining air volumes (and particles) are assumed to pass around the column in streamline flow.

The conditions for interaction are illustrated in Figure 5 for a given altitude of interaction. The differential cross section for interaction is given by

$$\frac{d\sigma}{d\theta} = \frac{U\cos\theta}{U_0}, \quad U\cos\theta < U_0 \tag{22}$$

where U is the characteristic radial plume velocity at the boundary and U_0 is the ambient wind velocity. It is assumed that the cross section for interaction is unity when $U\cos\theta \geq U_0$.

Differential particle escape probabilities are given by

$$P_e(\theta) = 1 - \frac{U\cos\theta}{U_0}, \quad U\cos\theta < U_0 \tag{23}$$

and

$$P_e(\theta) = 0 \quad , U\cos\theta \geq U_0 \tag{24}$$

For several wind structures, the escape probabilities for particles are given in Tables 1 and 2. They are given in terms of $P_e(\ell)$ where $P_e(\ell)$ is given by $1 - (U/U_o)\,[R^2(Z)-\ell^2]^{1/2}/R(Z)$ for the conditions of Equation 23, where R(Z) is the plume radius at Z, and where ℓ is the perpendicular distance from the center line formed by the plume and the ambient wind (see Figure 5). Under the ambient wind and fire conditions of Table 1, for plume heights between 700 to 3,000 feet, almost all fallout particles directed toward it would interact with the plume. Upon interacting, spherical particles of 2.5 gm/cm^3 density and 1,000 μ diameter would be swept up to 6,600 feet, of 600 μ diameter to 10,900 feet, and all smaller particles to the top of the column, from which they begin falling earthward again. The heights to which particles of different diameters may rise in plumes generated under a variety of fire conditions are given in Table 3.

In Table 2, the wind velocity is varied linearly with height from a surface wind of 5 miles per hour along a line that intersects average mid-latitude summer wind values at 10 kilometer altitude[15] (the extropolation of the linear relationship so obtained to higher altitudes probably, on the average, would give an over-estimate of the true wind speeds at these altitudes). As shown in Table 2, the effect of higher wind velocities at the higher altitudes is to decrease the shadowing effect evident at low average wind velocities.

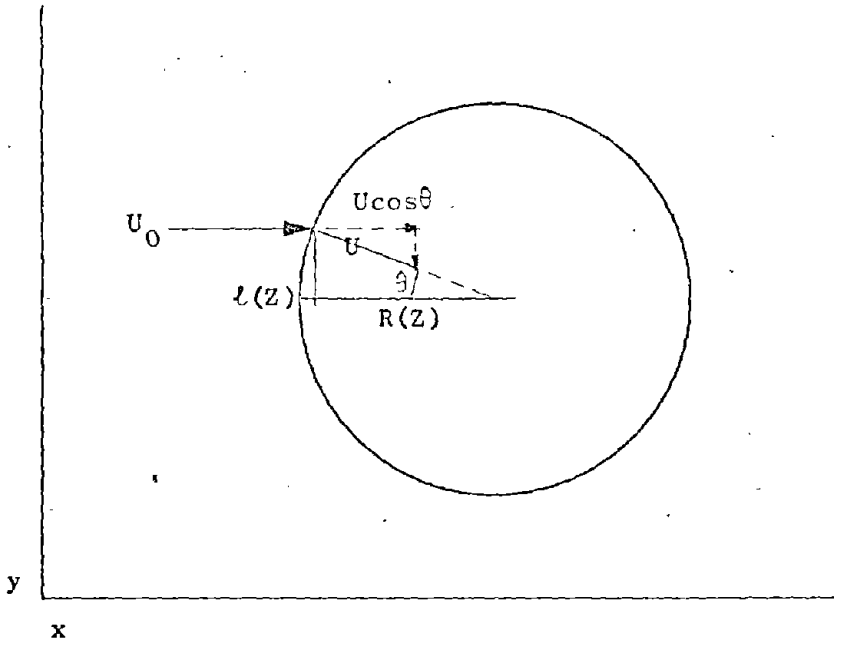

Fig. 5. Wind Interaction Parameters

Table 1

PARTICLE ESCAPE PROBABILITIES, $P_e(\ell)$

Constant Horizontal Wind of 5 mph (7.33 ft/sec), R = 5,000 ft, $F = 1 \times 10^{-4}$ lbs/ft^2-sec, ℓ in Feet

Z (ft)	U $\left(\frac{ft}{sec}\right)$	R(z) (ft)	$P_e(\ell)$										
			$\ell = 0$	$\ell = 50$	$\ell = 100$	$\ell = 150$	$\ell = 200$	$\ell = 250$	$\ell = 300$	$\ell = 350$	$\ell = 400$	$\ell = 450$	$\ell = 500$
0	0	5,000	-	-	-	-	-	-	-	-	-	-	-
100	2.17	532	0.704	0.705	0.709	0.716	0.726	0.739	0.756	0.777	0.805	0.842	0.899
200	3.28	271	0.553	0.560	0.584	0.627	0.714	0.827	1	1	1	1	1
300	5.30	265	0.277	0.290	0.330	0.404	0.526	0.760	1	1	1	1	1
400	6.83	277	0.068	0.084	0.131	0.217	0.355	0.599	1	1	1	1	1
700	7.81	313	0	0	0	0.065	0.180	0.359	0.696	1	1	1	1
1,000	10.03	348	0	0	0	0	0	0.048	0.307	1	1	1	1
1,500	10.21	407	0	0	0	0	0	0	0.059	0.289	0.743	1	1
2,000	10.06	466	0	0	0	0	0	0	0	0.094	0.296	0.643	1
3,000	9.12	584	0	0	0	0	0	0	0	0.004	0.093	0.207	0.357
5,000	6.61	820	0.098	0.100	0.105	0.113	0.125	0.141	0.161	0.184	0.213	0.246	0.285
7,500	4.60	1,115	0.372	0.373	0.375	0.378	0.383	0.388	0.396	0.404	0.414	0.426	0.439
10,000	3.49	1,410	0.524	0.524	0.525	0.527	0.529	0.531	0.535	0.539	0.543	0.549	0.555
15,000	2.36	2,000	0.678	0.678	0.678	0.679	0.680	0.681	0.682	0.683	0.685	0.686	0.688
20,000	1.78	2,590	0.757	0.757	0.757	0.758	0.758	0.758	0.759	0.760	0.761	0.762	0.763
30,000	1.19	3,770	0.838	0.838	0.838	0.838	0.838	0.838	0.838	0.838	0.839	0.839	0.839

Table 2

PARTICLE ESCAPE PROBABILITIES, $P_e(\ell)$
Horizontal Surface Wind of 5 mph (7.33 ft/sec)*, F = 1×10^{-4} lbs/ft^2-sec, ℓ in Feet

Z (ft)	U $\left(\frac{ft}{sec}\right)$	U_0 $\left(\frac{ft}{sec}\right)$	R(z) (ft)	$P_e(\ell)$										
				$\ell = 0$	$\ell = 50$	$\ell = 100$	$\ell = 150$	$\ell = 200$	$\ell = 250$	$\ell = 300$	$\ell = 350$	$\ell = 400$	$\ell = 450$	$\ell = 500$
0	0	7.33	5,000	-	-	-	-	-	-	-	-	-	-	-
100	2.17	7.64	532	0.716	0.717	0.721	0.727	0.736	0.749	0.765	0.786	0.812	0.849	0.903
200	3.28	7.95	271	0.587	0.595	0.617	0.656	0.722	0.841	1	1	1	1	1
300	5.30	8.25	265	0.358	0.364	0.405	0.470	0.578	0.787	1	1	1	1	1
400	6.83	8.56	277	0.202	0.215	0.256	0.329	0.448	0.656	1	1	1	1	1
700	7.81	9.49	373	0.177	0.184	0.207	0.246	0.305	0.389	0.511	0.715	1	1	1
1,000	10.03	10.41	348	0.037	0.047	0.077	0.131	0.212	0.330	0.512	0.640	1	1	1
1,500	10.21	11.95	407	0.146	0.152	0.172	0.206	0.256	0.326	0.423	0.564	0.839	1	1
2,000	10.06	13.49	466	0.254	0.259	0.272	0.294	0.326	0.371	0.429	0.507	0.617	0.806	1
3,000	9.12	16.57	584	0.450	0.452	0.458	0.468	0.483	0.503	0.528	0.559	0.598	0.649	0.715
5,000	6.61	22.73	820	0.709	0.710	0.711	0.714	0.718	0.723	0.729	0.737	0.746	0.756	0.769
7,500	4.60	30.43	1,115	0.849	0.849	0.849	0.850	0.851	0.853	0.854	0.857	0.859	0.862	0.865
10,000	3.49	38.13	1,410	0.908	0.909	0.909	0.909	0.909	0.909	0.911	0.911	0.912	0.913	0.914
15,000	2.36	53.53	2,000	0.956	0.956	0.956	0.956	0.956	0.956	0.956	0.957	0.957	0.957	0.958
20,000	1.78	68.93	2,590	0.974	0.974	0.974	0.974	0.974	0.974	0.974	0.974	0.974	0.975	0.975
30,000	1.19	99.73	3,770	0.988	0.988	0.988	0.988	0.988	0.988	0.988	0.988	0.988	0.988	0.988

* $U = 7.33 + 3.08 \times 10^{-3}Z$, Z in feet

Table 3

RISE HEIGHTS ATTAINED BY PARTICLES OF DIFFERENT DIAMETERS THAT ENTER THE PLUME (in 10^3 feet)

R (ft)	40 μ	60 μ	120 μ	200 μ	400 μ	600 μ	1,000 μ	F $\left(\frac{\text{lbs}}{\text{ft}^2\text{-sec}}\right)$
1,000	31.0	31.0	23.0	12.7	6.0	3.9	2.3	1×10^{-3}
2,000	44.0	44.0	44.0	35.8	17.6	11.8	7.1	1×10^{-3}
3,000	54.0	54.0	54.0	54.0	29.1	19.8	12.4	1×10^{-3}
4,000	62.0	62.0	62.0	62.0	39.0	27.0	17.2	1×10^{-3}
5,000	69.0	69.0	69.0	69.0	47.3	33.1	21.4	1×10^{-3}
6,000	76.0	76.0	76.0	76.0	54.3	38.3	25.1	1×10^{-3}
7,000	82.0	82.0	82.0	82.0	60.1	42.6	28.2	1×10^{-3}
8,000	88.0	88.0	88.0	88.0	65.1	46.4	30.9	1×10^{-3}
9,000	93.0	93.0	93.0	93.0	69.4	49.6	33.3	1×10^{-3}
10,000	98.0	98.0	98.0	98.0	73.2	53.5	35.4	1×10^{-3}
1,000	17.5	16.1	6.2	3.4	1.6	1.0	0.55	1×10^{-4}
2,000	24.7	24.7	19.2	10.6	5.0	3.2	1.9	1×10^{-4}
3,000	30.2	30.2	30.2	18.7	8.9	5.9	3.5	1×10^{-4}
4,000	34.9	34.9	34.9	26.4	12.8	8.5	5.1	1×10^{-4}
5,000	39.0	39.0	39.0	33.4	16.3	10.9	6.6	1×10^{-4}
6,000	42.8	42.8	42.8	39.6	19.5	13.1	8.0	1×10^{-4}
7,000	46.2	46.2	46.2	45.0	22.3	15.1	9.2	1×10^{-4}
8,000	49.4	49.4	49.4	49.4	24.8	16.8	10.4	1×10^{-4}
9,000	52.4	52.4	52.4	52.4	27.0	18.4	11.4	1×10^{-4}
10,000	55.2	55.2	55.2	55.2	29.0	19.8	12.3	1×10^{-4}

The general circumstances under which fallout – fire interactions may take place includes all combinations of air burst detonations over a target area with fallout arriving from other upwind detonations. The special conditions where a surface burst is the source of fire ignitions as well as the source of the fallout is examined in the following paragraphs.*

For conditions appropriate to surface detonations of weapons of a number of yields, source (cloud) mid-heights vary according to the relation of Miller.[16]

$$z_o = 1.68 \times 10^4 \, W^{0.164} \quad ; \; 30 \leq W \leq 100{,}000 \text{ KT} \tag{25}$$

In Equation 25, z_o is given in feet, with W representing the total weapon yield in kilotons. Thus, source mid-height cloud location at the time of its formation (in this treatment: zero time) is estimated.

Upon detonation of a nuclear weapon, a great deal of energy is, of course, released in the form of thermal energy, and the distances from the point of detonation to the limits of ignitions can be reasonably estimated. LaRiviere and Lee[17] have derived relations from which expected radiant energy fluxes with distance from a surface burst as a function of weapon yield may be estimated. Under average atmospheric conditions, the distance from a surface burst where thermal fluxes decrease to the 8-calorie-per-cm^2 level is given by

$$S = 687.2 \, W^{1/2} \tag{26}$$

where S is the horizontal distance from the detonation in feet. The distance at which the 8 calorie per cm^2 level of radiant energy flux occurs was taken to be the limiting distance from the detonation for fire start. The use of an 8 calorie per cm^2 flux level for an ignition limit is based on data given

---

* The case where the fallout arrives prior to ignition of a fire is not considered here; exploratory investigations have indicated redistribution but not removal effects for fallout deposited prior to fire ignition.

in the Effects of Nuclear Weapons.[18] It is the lower limit for ignition of highly inflammable materials. In some cases,[19] levels as high as 50 calories per cm^2 are judged to be required for fire start.

While fires may be initiated out to the distances given above, experience obtained from incendiary bombing raids indicate that a time lapse occurs between the time of fire start to the time when massive fires can be burning. Estimates of the length of this period may vary from approximately 25 to 45 minutes on the basis of descriptions of German experience in World War II.[20]

All the above factors are synthesized into Figures 6 through 11, which show the origins of several detonations, cloud mid-heights, trajectories as functions of particle size, limits of ignition, and cloud positions at times when massive fires could be in progress. The figures are descriptive of the differences between detonations of widely different yields. The development of fire plumes that might be caused by a 30-KT weapon, occurs too late in time under most conceivable situations to significantly affect the fallout deposition pattern from the same event. On the other hand, a 10-MT surface burst moves the limits of ignition out to substantial distances from the point of detonation. In addition, since cloud mid-height is not highly sensitive to weapon yield (i.e., $z_o = 1.68 \times 10^4 \, W^{0.164}$), the probability of fallout — fire interactions is much greater for the higher yield weapons under the same atmospheric conditions.

The deposition patterns that would result from plume interactions with fallout particles of a number of diameters under specified wind and fire conditions are shown in Figures 12 through 16. In the figures, ρ/ρ_0 is the ratio of the fallout density resulting from fire plume interactions, ρ, to the density, ρ_0, expected in the absence of the fire; and the wind speed, U_0, was taken to be the same for all Z. Fallout deposition in the shadow of the plume is especially sensitive to the value of the ambient wind speed, U_0. Substantial plume — fallout interactions are indicated for low wind speed conditions resulting in a large degree of "shadowing" by the plume in the downwind region. Increases in fire diameter or intensity also result in increases in the interaction of fallout with the plume. The material that interacts with or enters the plume is carried aloft to altitudes as given in Table 3, from which it again begins its descent.

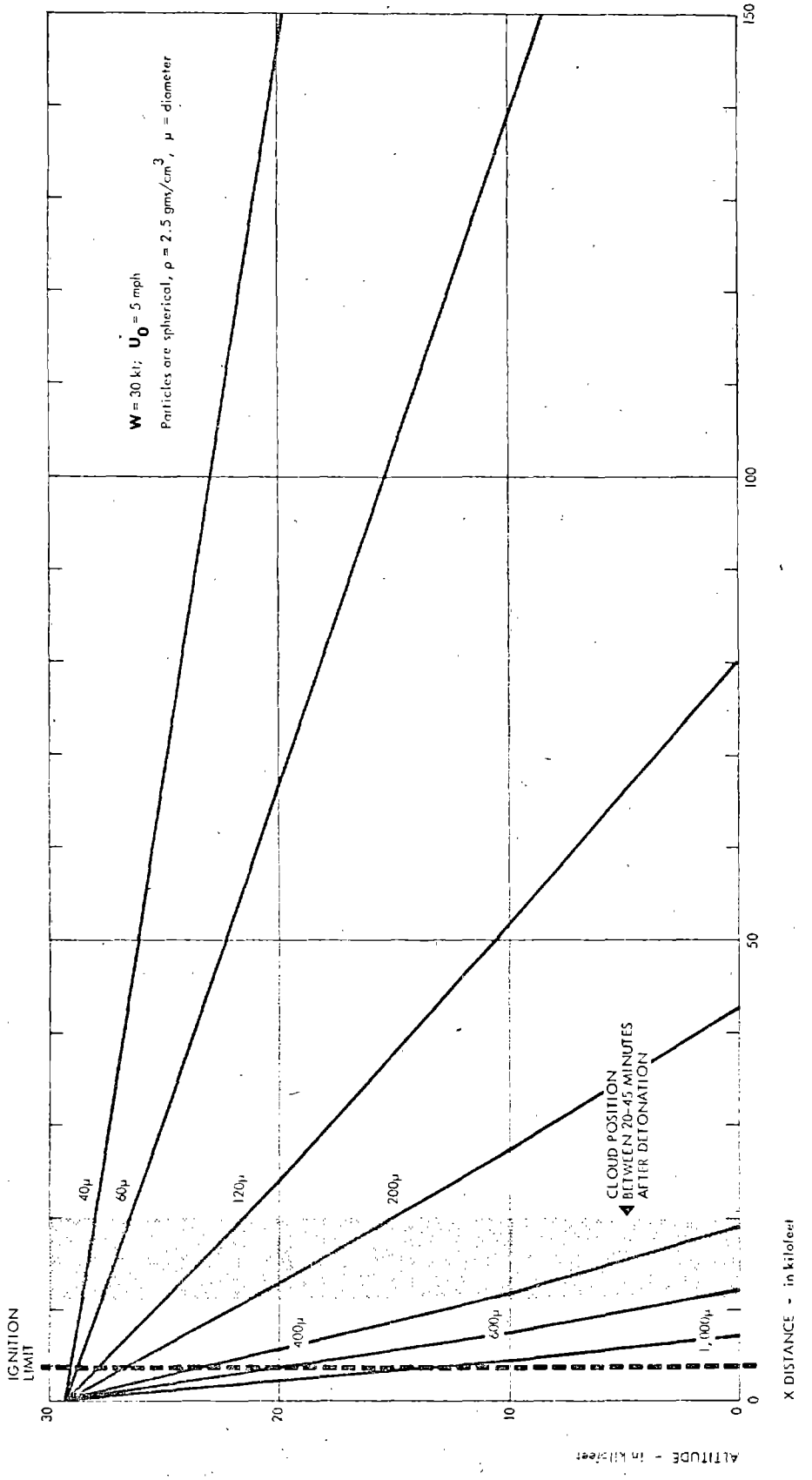

Fig. 6. Particle Trajectories and Fire Conditions.

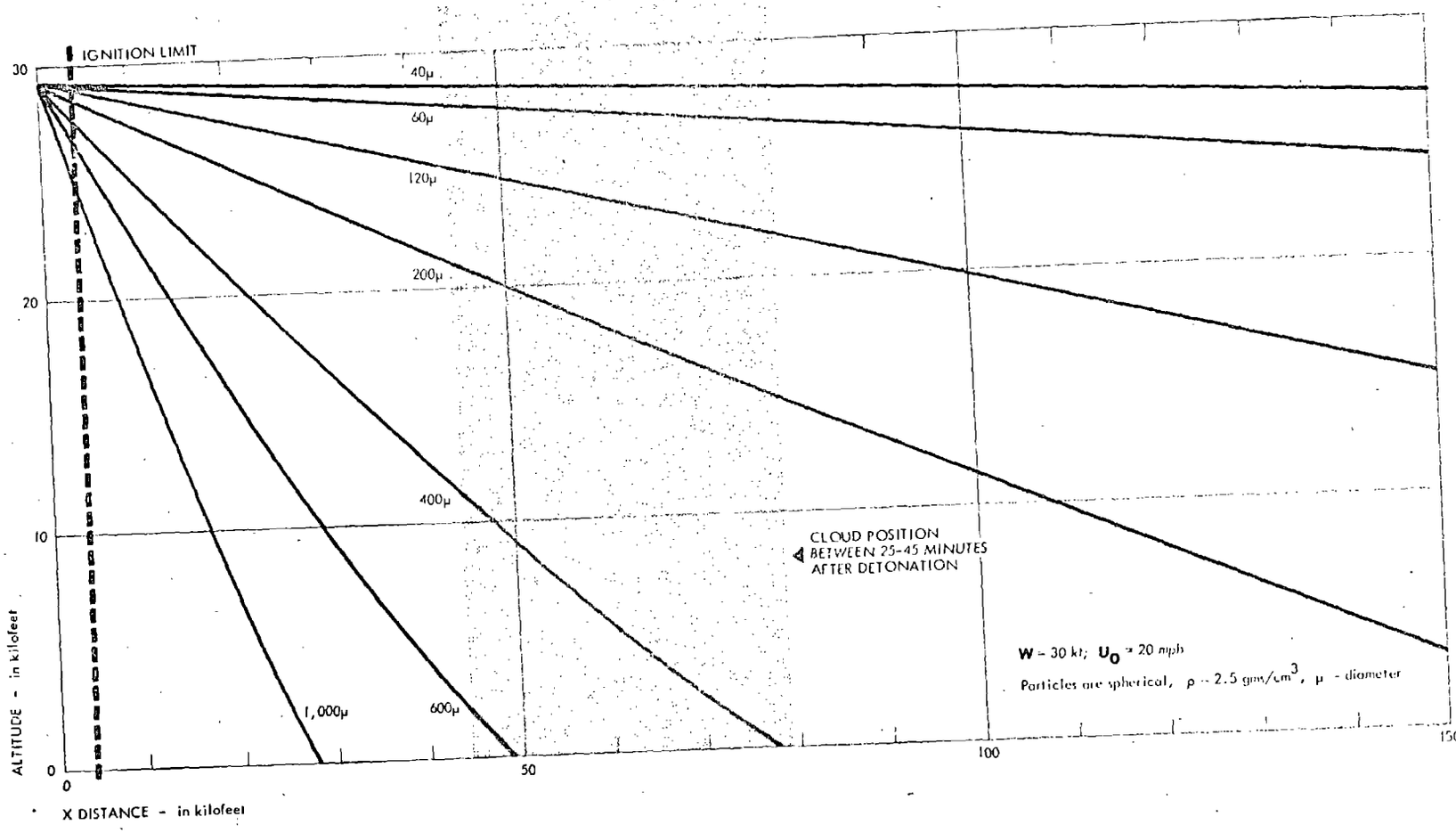

Fig. 7. Particle Trajectories and Fire Conditions.

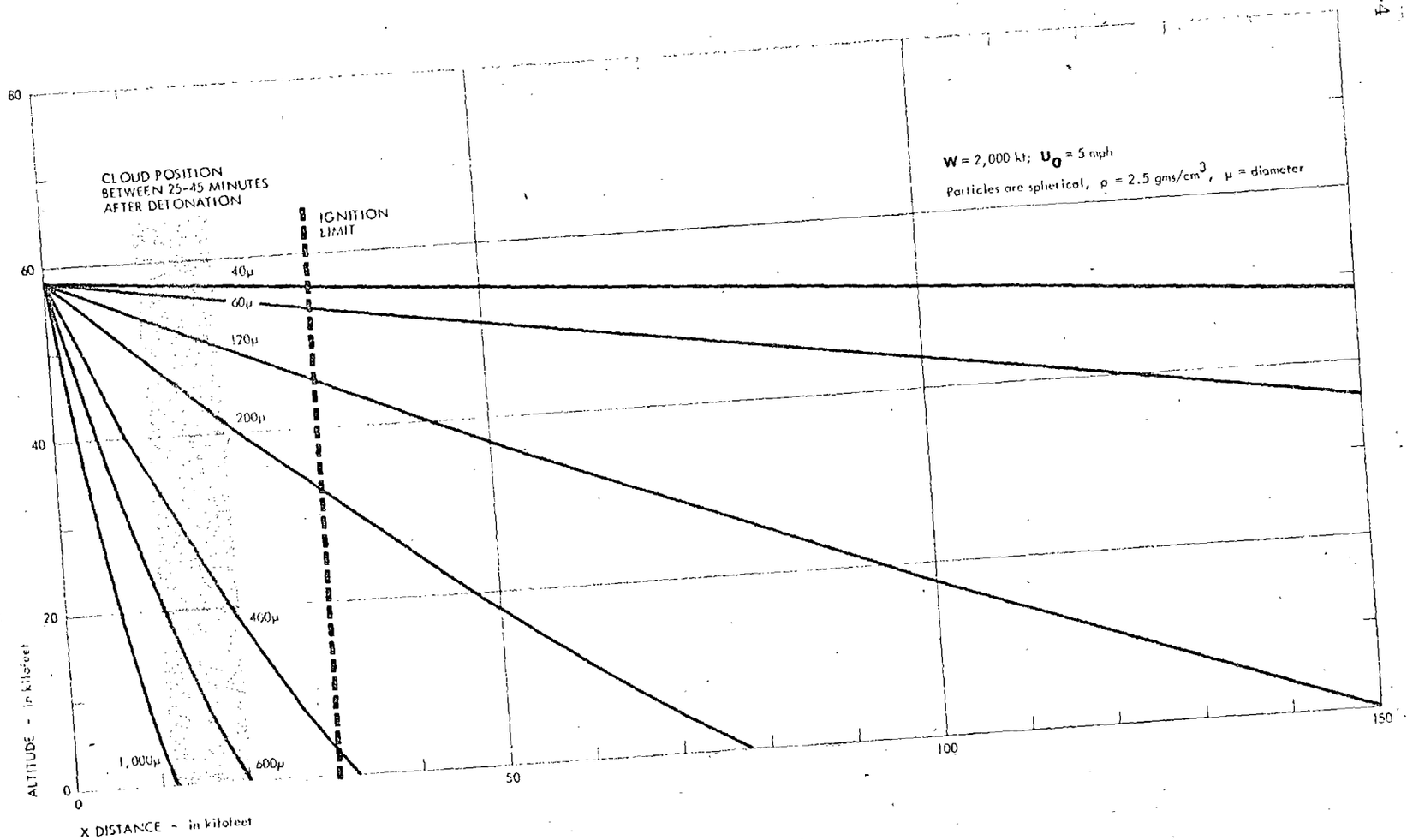

Fig. 8. Particle Trajectories and Fire Conditions.

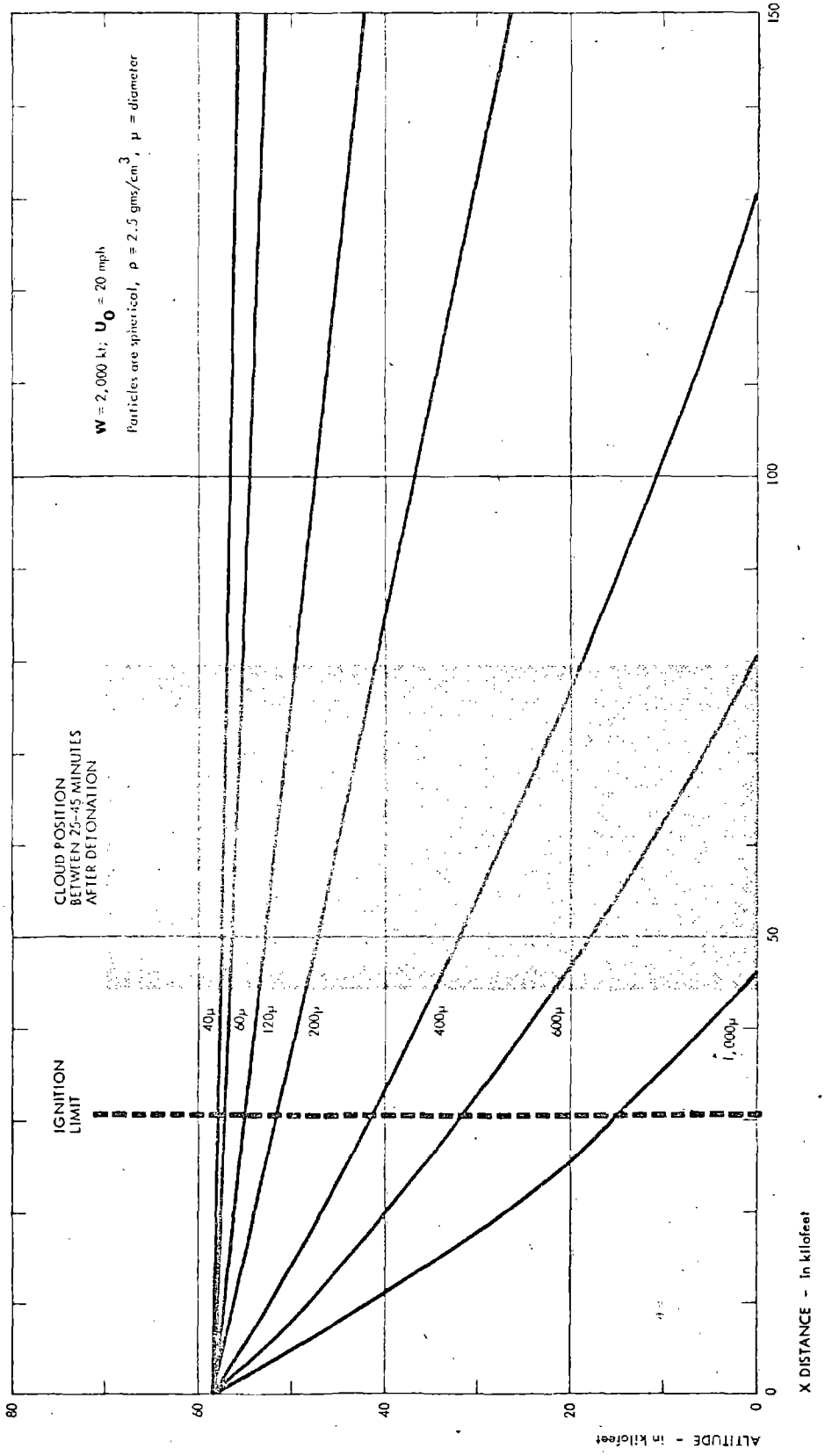

Fig. 9. Particle Trajectories and Fire Conditions.

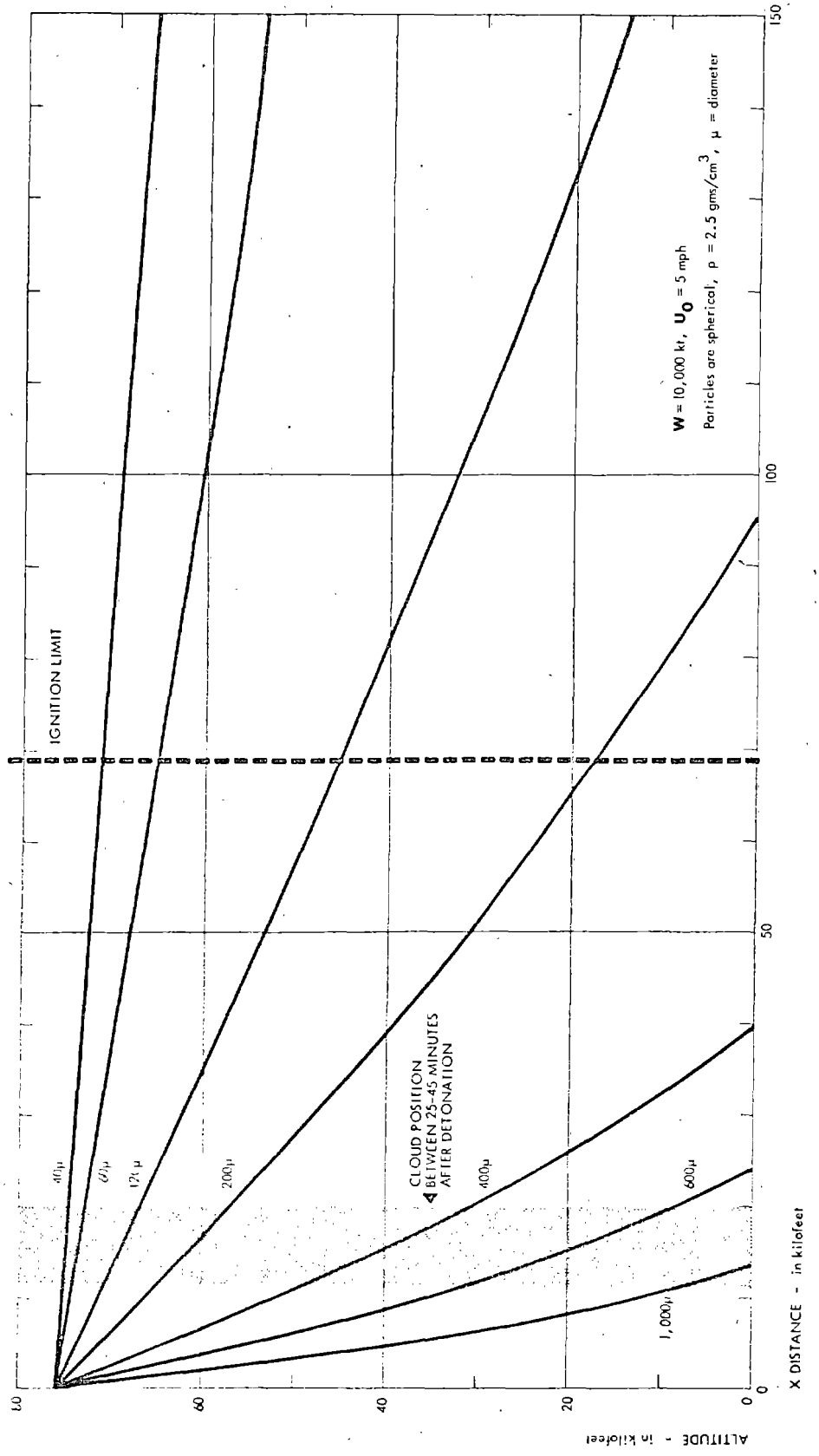

Fig. 10. Particle Trajectories and Fire Conditions.

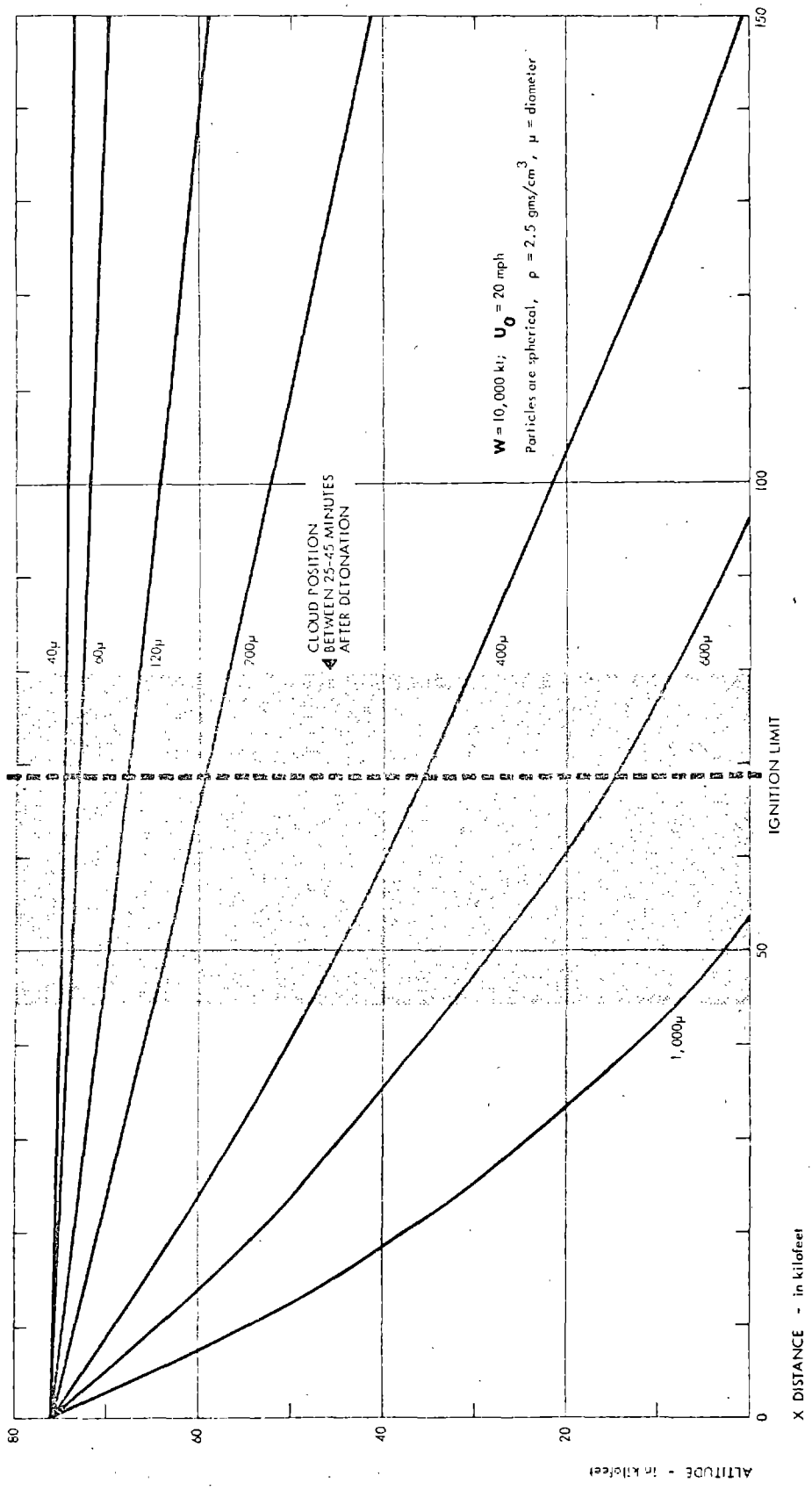

Fig. 11. Particle Trajectories and Fire Conditions.

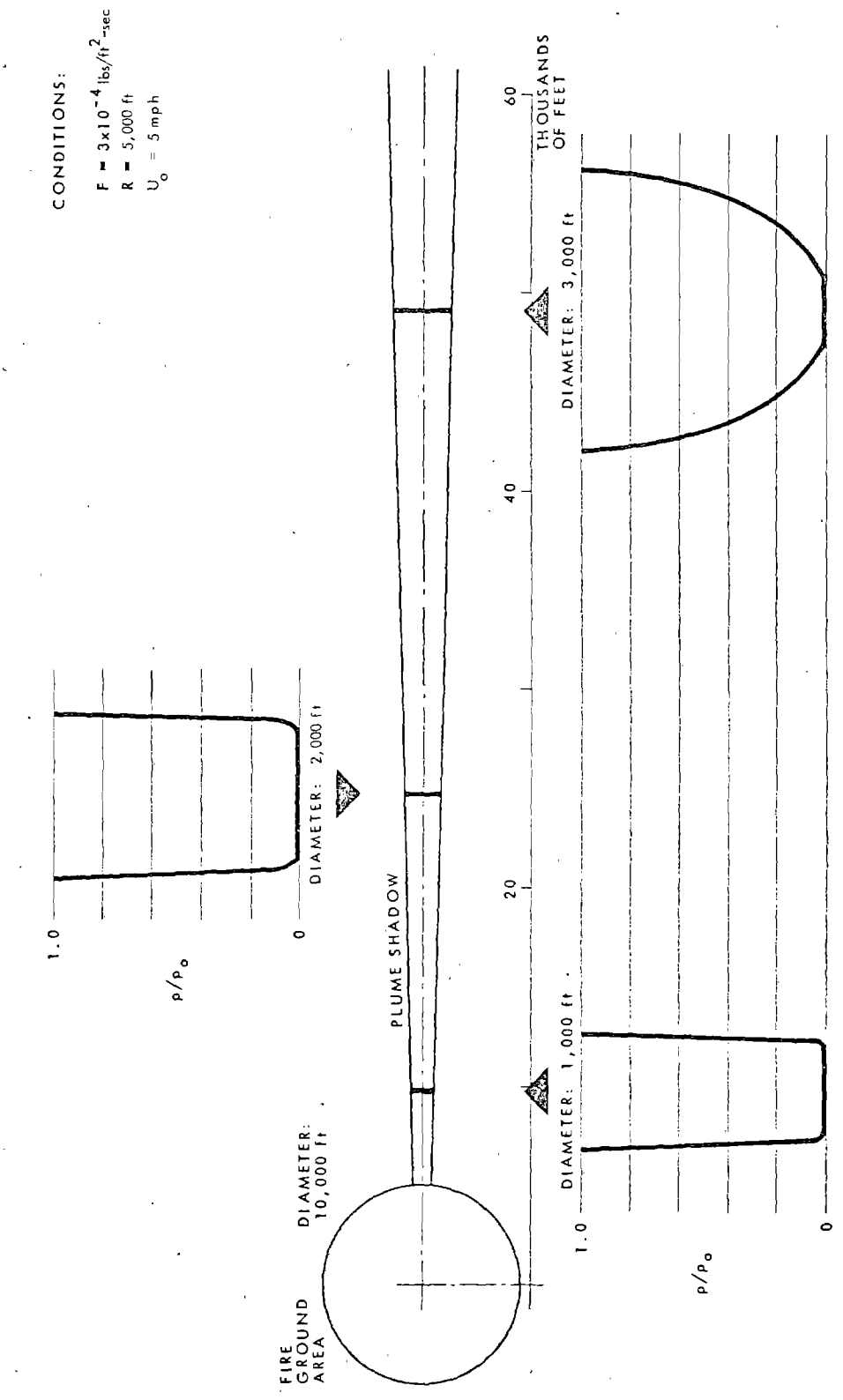

Fig. 12. Deposition Patterns: 80-μ-Diameter Spheres

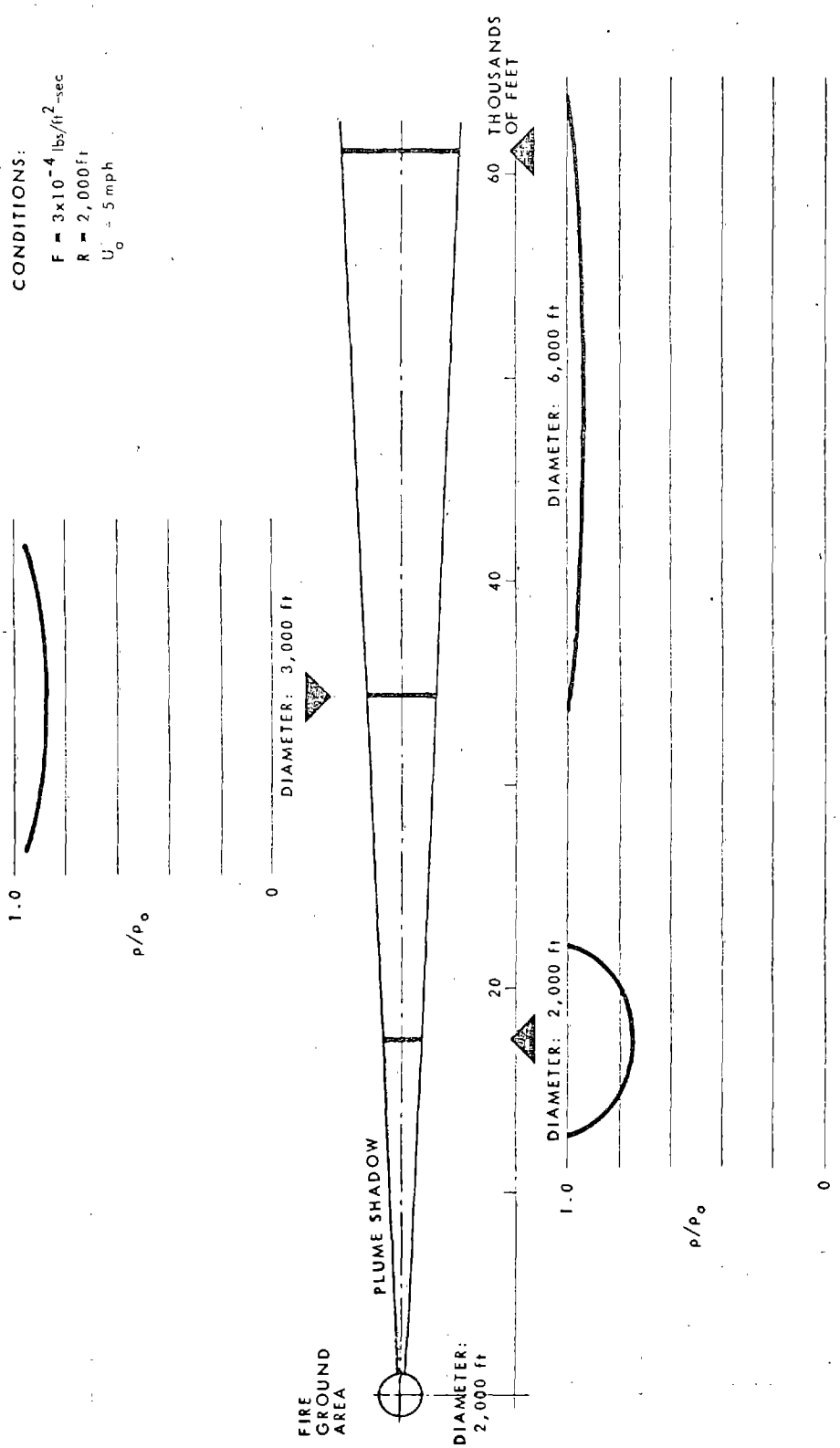

Fig. 13. Deposition Patterns: 200-μ-Diameter Spheres

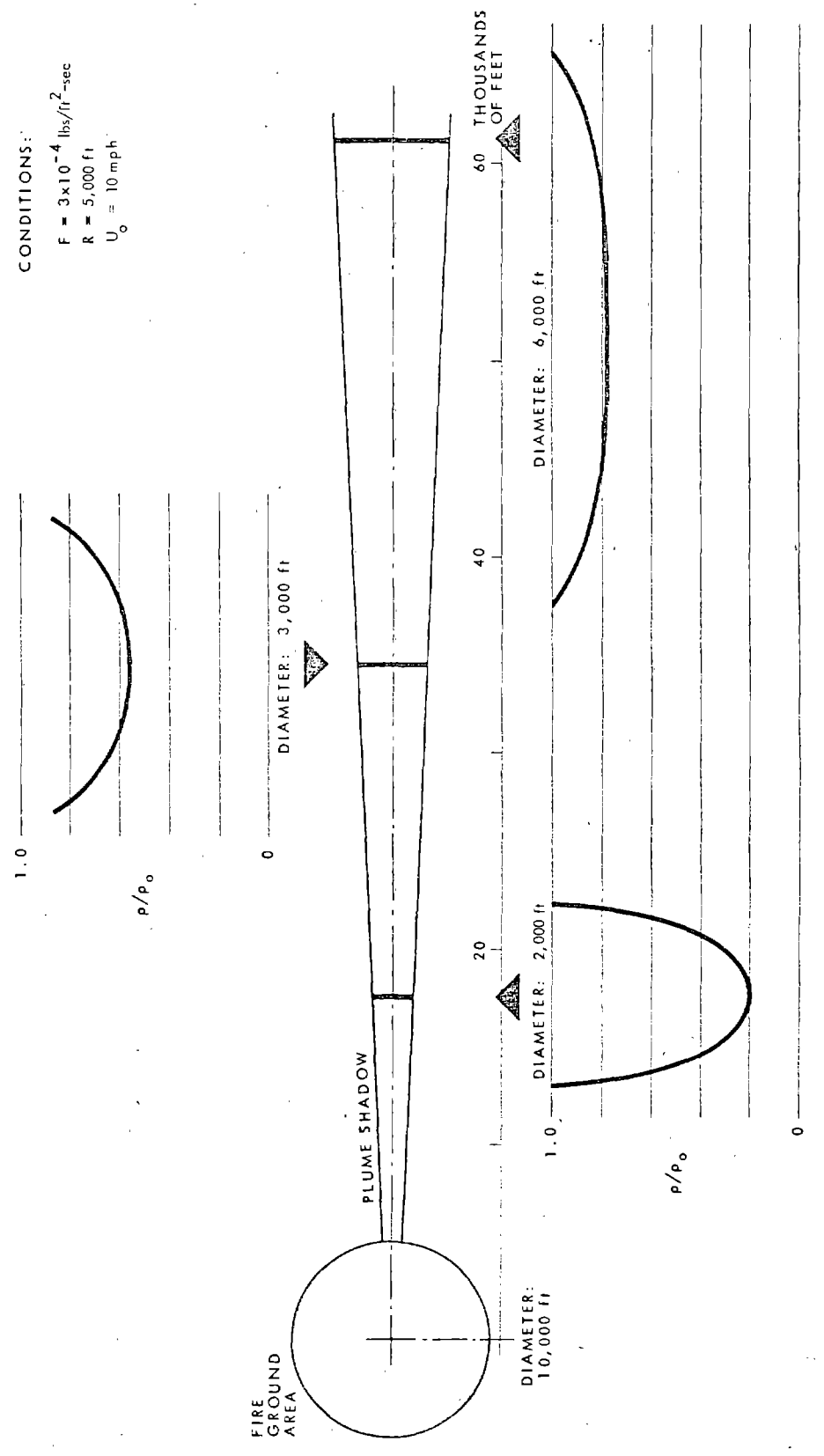

Fig. 14. Deposition Patterns: 200-μ-Diameter Spheres

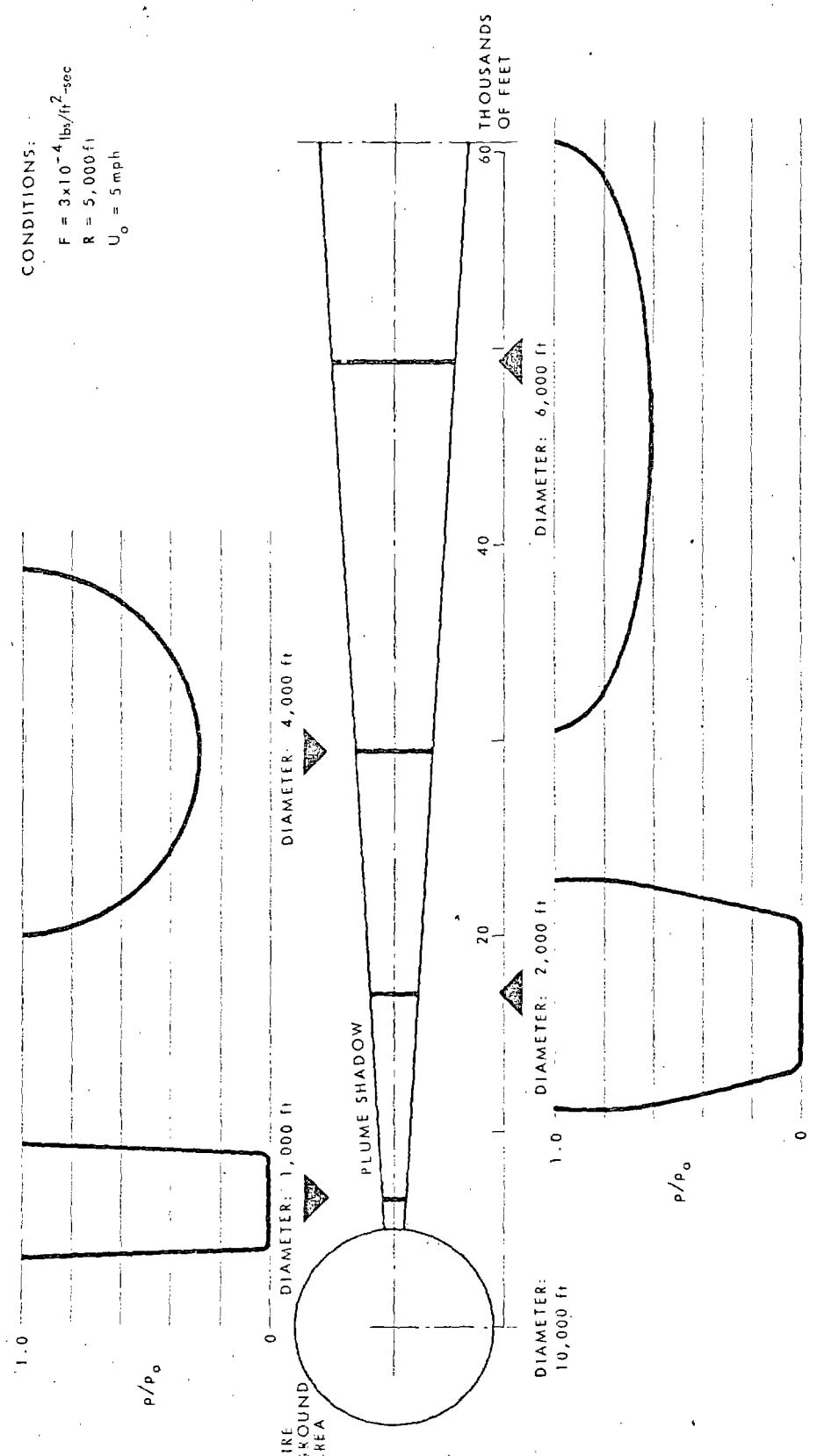

Fig. 15. Deposition Patterns: 150-μ-Diameter Spheres

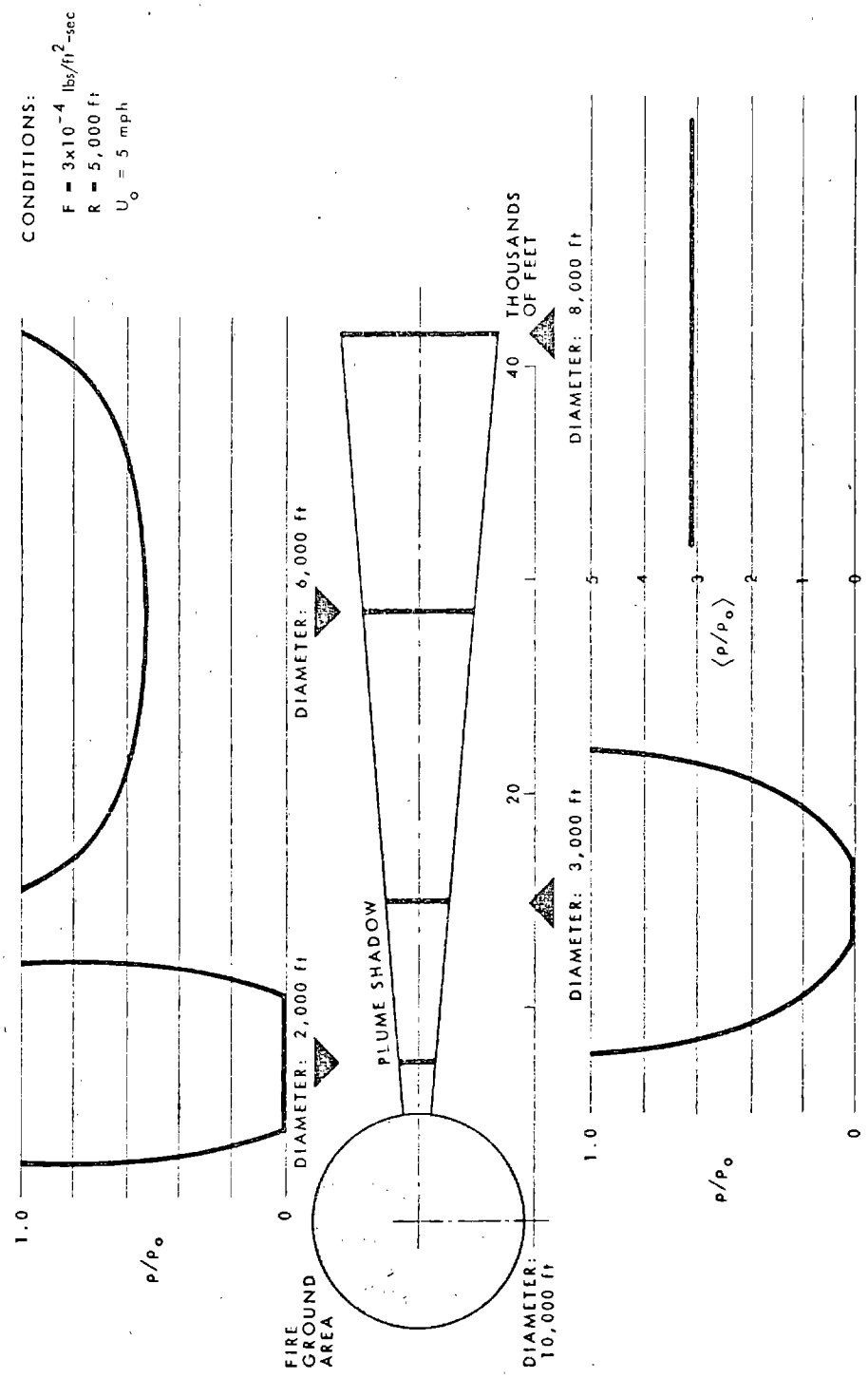

Fig. 16. Deposition Patterns: 200-μ-Diameter Spheres

If no lateral mixing occurs in the plume for a uniform air concentration of the incident fallout, the relative density distribution of particles in the plume cross section perpendicular to the wind direction can be estimated from the capture probabilities as functions of altitude for constant values of ℓ (see Figure 5). The relation

$$(\rho/\rho_0)_{H,\ell} = \int_0^H q(\ell,Z)dZ \tag{27}$$

represents the relative quantity of particles raised to the equilibrium altitude, H, in the plume at the distance, ℓ, from the fire center perpendicular to the wind. The distribution given in Figure 17 applies in general to the conditions given in Figures 12, 13, 15, and 16, for captured particles that rise to 30,000 feet. The equation

$$(\rho/\rho_0)_H = 12.3\ e^{-\ 0.00082|\ell|} \tag{28}$$

is a least squares representation of the points across ℓ determined from Equation 27. In Equation 28, ℓ is given in feet. Since the particles in the plume are assumed to be uniformly mixed, at a given value of ℓ, the value for deposition density is then given by:

$$\left\langle \rho/\rho_0 \right\rangle = \frac{\int_0^{R(Z)} a\ell e^{-\ b\ell} d\ell}{\int_0^{R(Z)} \ell d\ell} \tag{29}$$

where R(Z) is the radius of the plume at the altitude, H, ρ/ρ_0 is the average value of relative deposition density across the plume at altitude, H, and a is the coefficient appropriate to the altitude, H. If fallout were deposited and redeposited from the top of the plume, the relation becomes:

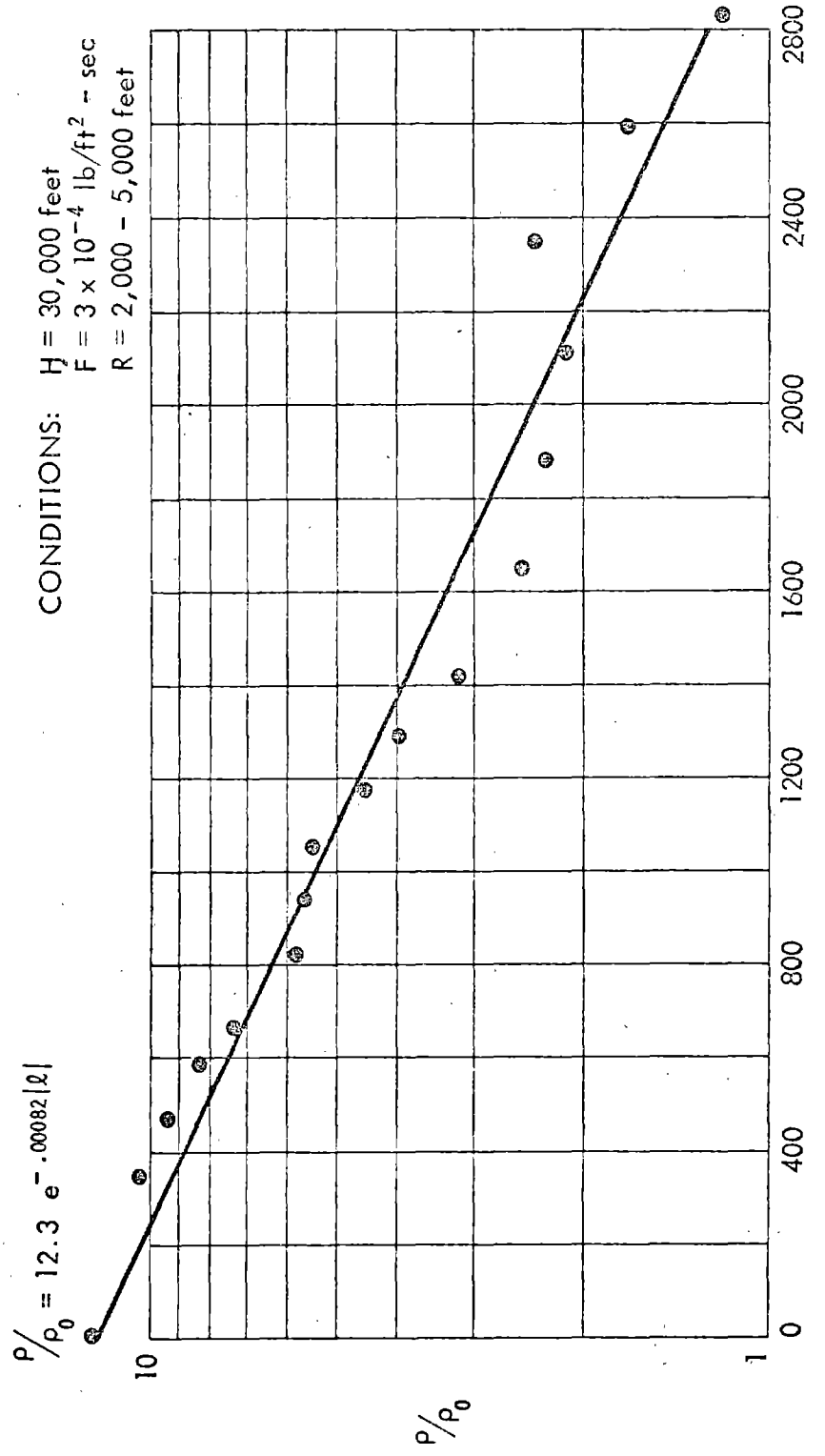

Fig. 17. Relative Distribution of Particles Under Nonturbulent Plume Conditions.

$$\left\langle \rho/\rho_0 \right\rangle = 1 + \frac{\int_0^{R(Z)} a\ell e^{-b\ell} d\ell}{\int_0^{R(Z)} \ell d\ell} \tag{30}$$

since normal deposition also would occur from that altitude.

The overall cross section for interaction of the plume may be estimated through the following relations:

Plume radius as a function of altitude may be represented by

$$R(Z) = (R - 230)e^{-0.028Z} + 0.118Z + 230 \tag{31}$$

where R(Z) is the radius in feet,

R is the ground radius in feet, and

Z is the height in feet.

The overall interaction cross section for the plume to the altitude H is defined by

$$\sigma = \frac{\int_0^H \int_0^{\pi/2} R(Z)\left(\frac{d\sigma}{d\vartheta}\right)\cos\vartheta \; dz \; d\vartheta}{\int_0^H \int_0^{\pi/2} R(Z)\cos\vartheta \; dz \; d\theta} \tag{32}$$

Total plume interaction probabilities and interaction probabilities for altitude increments under a variety of environmental and fire conditions are presented in Table 4. As expected, the principal region of the plume where interactions take place is in the low-altitude portion, where radial wind velocities are highest.

Table 4

PLUME INTERACTION PROBABILITIES

Ambient Wind Velocity U_0	Fire Radius R	Gas Generation Rate, F	Interaction Probabilities For Altitude Increments, σ										
			0-5,000	5,000-10,000	10,000-15,000	15,000-20,000	20,000-25,000	25,000-30,000	30,000-35,000	35,000-40,000	40,000-45,000	45,000-50,000	Entire Plume
7.33	2,000	1×10^{-4}	0.37	0.13	0.073	0.049	-	-	-	-	-	-	0.081
14.67	5,000	1×10^{-4}	0.44	0.23	0.13	0.088	0.064	0.049	0.039	0.031	-	-	0.078
22.00	5,000	3×10^{-4}	0.40	0.28	0.17	0.11	0.083	0.063	0.050	0.040	0.032	0.026	0.067

One illustrative set of calculations was carried out to investigate the effect of a large-scale fire on fallout patterns; in this calculation a surface detonation with a weapon yield of 1 MT (25 percent fission) was selected along with the fire condition parameter values given in Figures 12 through 16. Values of these parameters and others for the fallout pattern[16] are summarized in Table 5 for each of the five case situations that follow from Figures 12 through 16. No information appears to be directly available regarding the possibility of feasibility of occurrence of the paired values of R and F used in the calculations. The values of U_0 used in the calculations cannot be said to have a very significant probability of occurrence. U_0 was taken to be the same at all Z; F was assumed to remain constant over the whole fallout period.

In the calculations, the value of d refers to a mid-range particle diameter representing particles originating at the center-height of the cloud directly over ground zero. The downwind distance to the fire, X_F, was estimated by letting the particles with diameter $\bar{d}$ originating from the cloud center intersect the plume at a height equal to one-half the height, Z_d, to which the particles would be lifted if they entered the plume. The particles that are recycled to Z_d would be carried farther downwind to the distance X_d from the center of the plume. No lateral or other diffusion of these particles was assumed and since an extremely narrow particle diameter distribution was also assumed, the added deposition would be in the form of a circular deposition pattern with radius R(Z) centered at X_d. To estimate I_d at $X_d \pm R(Z)$ along the pattern center line, values of $(1 - \rho/\rho_0)I_s$ along the pattern center line from $X_F - R$ to X_d were graphically integrated, divided by 2R(Z) and added to I_d^o, the calculated value of I_s at X_d for the no-fire case. The pattern profile from plume-lifted particles would, of course, become increasingly longer and asymmetrical as the range of diameters in the fallout particles that interact with the plume increases.

Table 5

SUMMARY OF ASSUMED AND DERIVED PARAMETERS FOR ESTIMATING EFFECTS ON FALLOUT PATTERN

CENTER-LINE I_s VALUES FROM A LARGE-SCALE FIRE DOWNWIND FROM A 1-MT YIELD SURFACE DETONATION[a]

QUANTITY	CASE 1	CASE 2	CASE 3	CASE 4	CASE 5
R (10^3 ft)	5	1	5	5	5
$\bar{d}$ (microns)	80	200	200	150	200
U_0 (mph)	5	5	10	5	5
X_F (miles)	26.2	9.7	15.8	12.6	8.3
Z_d (10^3 ft)	48.0	6.2	44.1	47.6	44.1
X_d (miles)	57.7	11.4	34.6	26.8	17.7
R(Z) (miles)	1.12	0.18	1.03	1.11	1.03
I_F^o (R/hr at 1 hr)	176	790	880	610	900
I_d^o (R/hr at 1 hr)	10	670	346	166	382
I_d (R/hr at 1 hr)	970	1,800	2,700	1,800	2,200

a. $F = 3 \times 10^{-4}$ lbs/sq ft-sec for all cases;
B = 0.25 (ratio of fission to total yield)

The resulting profiles of I_s as a function of distance along the pattern centerline are shown in Figure 18 for Cases 1 and 5 and in Figure 19 for Cases 2, 3, and 4. The largest relative effect on I_s is shown for Case 1 involving the particles with the smallest diameters; in the cited case, I_s values would be decreased by factors of 10 to 100 for a distance of about 15 miles from the downwind fire boundary; at a downwind distance of 58 ± 1 miles, the plume deposit would apparently produce an increase in I_s of about a factor of 100. The overall area of significant reduction in I_s between X_f and X_d is, however, not large; for Case 1, it is about 30 square miles. The area having increased values of I_s around X_d is estimated to be approximately 4 square miles in extent.

For Case 4 with $\bar{d}$ equal to 150 microns and Case 5 with $\bar{d}$ equal to 200 microns (all other conditions being the same as for Case 1), the downwind distance beyond the fire perimeter over which I_s is decreased becomes smaller and I_d becomes larger.

In the fire model, both the maximum vertical and horizontal velocities of the plume increase only in proportion to the 1/5-th power of the fuel gas generation rate, F. At small values of R, the fire radius, these two velocities increase almost directly with R (i.e. $R < 1{,}000$ ft) but tend to approach limiting values asymptotically as R becomes large (i.e. $R > 10{,}000$ ft). An arbitrary semi-empirical limit on the maximum plume height sets the maximum lateral dispersion of particles in the plume as increasing in proportion to $R^{\frac{1}{2}}F^{\frac{1}{4}}$; the calculated maximum downwind displacement of the smaller entrained particles at a given wind speed would be therefore directly proportional to $R^{\frac{1}{2}}F^{\frac{1}{4}}$. In general, the fire effects on displacement of the smaller particles are greater than they are for the larger particles. Higher horizontal wind velocities reduce the region of decreased deposition under the shadow of the plume and disperse the entrained particles to greater downwind distances; the higher wind speed thus could result in higher I_d/I_d^o ratios for fires at a given distance from the ground zero of the detonation which produces the fallout.

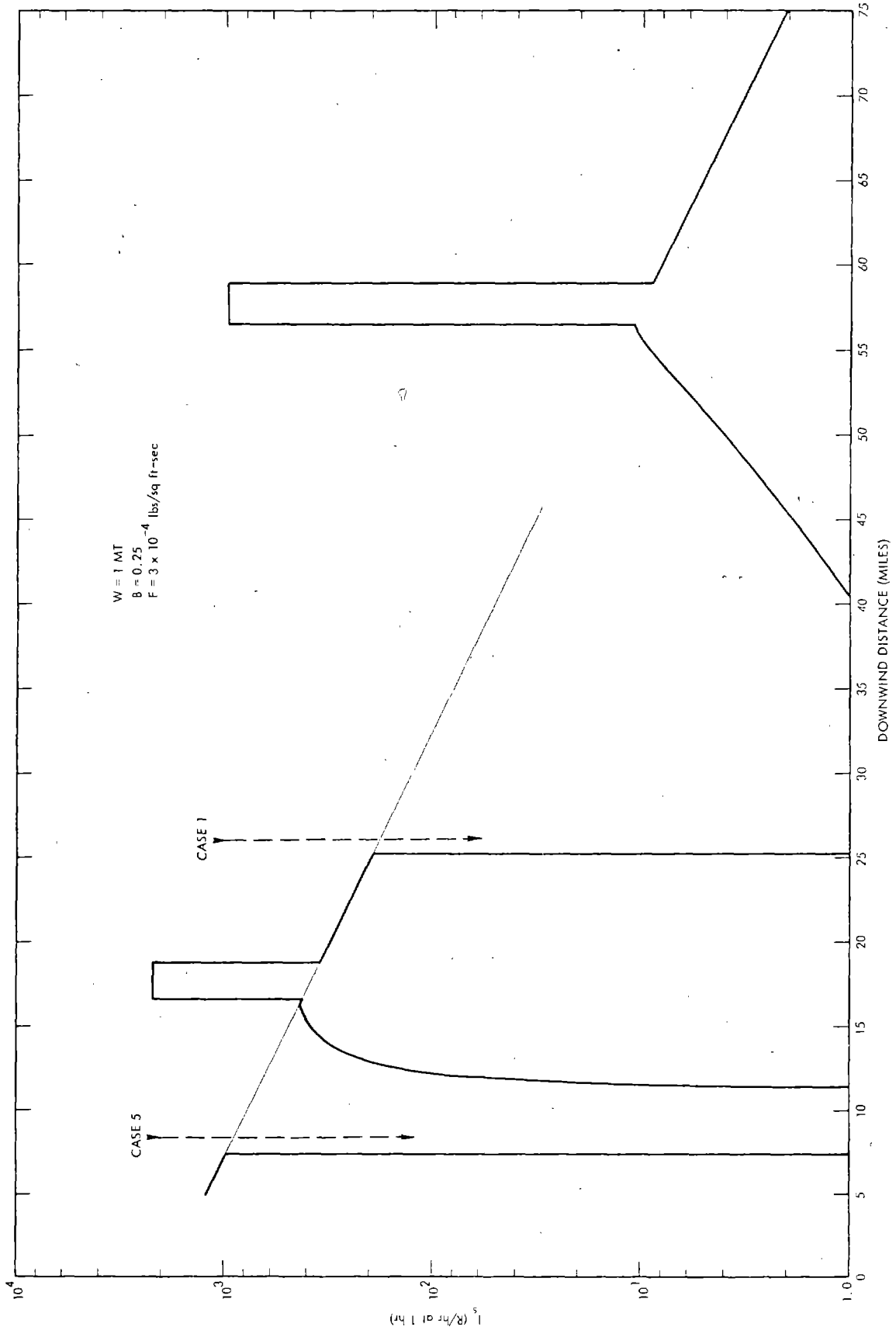

Fig. 18. Effect of Assumed Fires on the Variation of I_S with Distance Along the Fallout Pattern Centerline

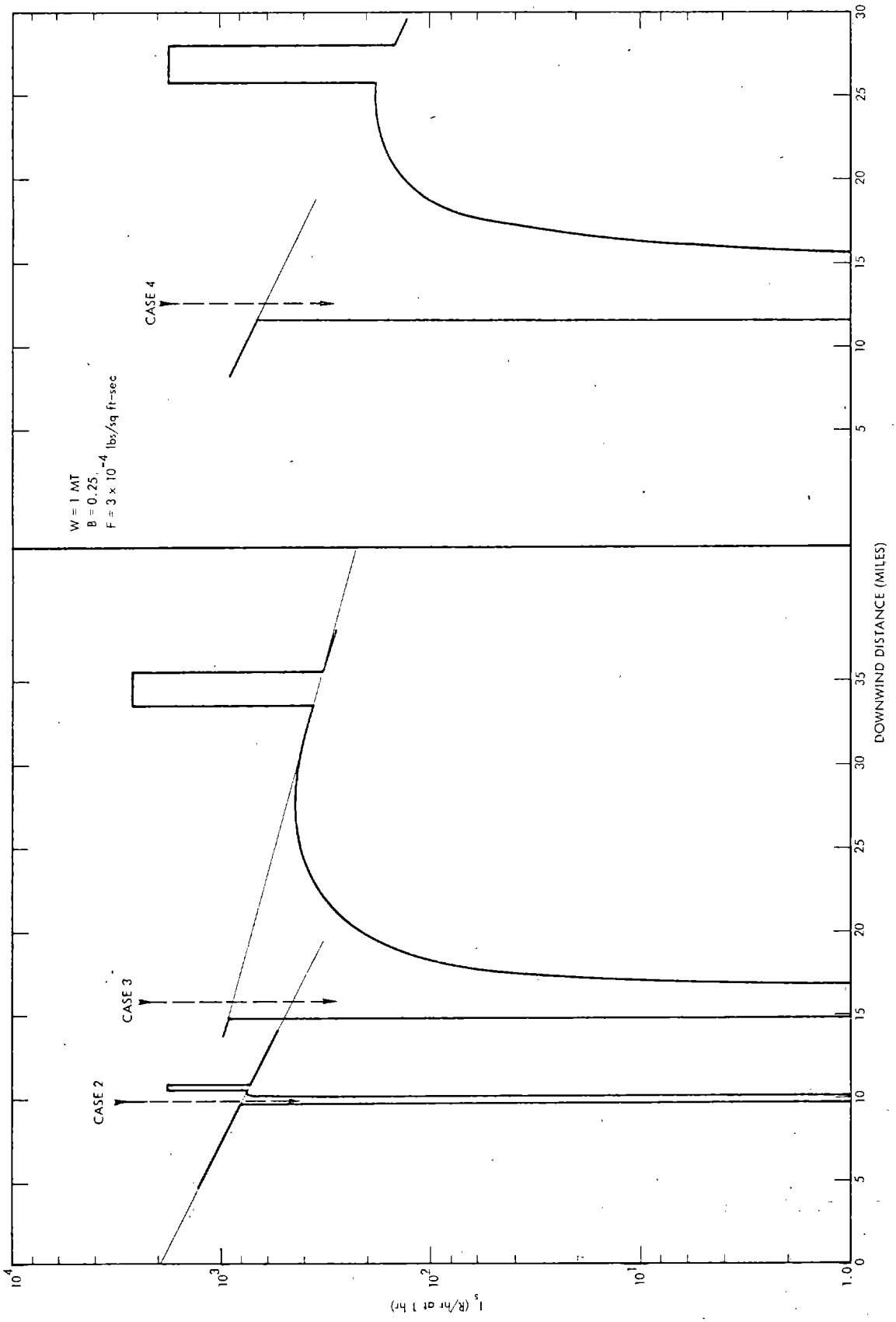

Fig. 19. Effect of Assumed Fires on the Variation of I_S with Distance Along the Fallout Pattern Centerline

Conclusions and Recommendations

Fallout patterns can be significantly altered by the existence of fire plumes that "shadow" areas that would otherwise be subject to fallout. The effects of "shadowing" are most marked for low ambient wind velocities at all altitudes, high gas generation rates, large fire areas, and small particles in the portion of the fallout cloud interacting with the plume. The principal effect of high gas generation rates and extensive fire area is to produce high inward-directed radial wind velocities in the plume at lower heights over the fire. Under these conditions, the interaction probabilities of fallout particles carried by ambient winds are increased. For constant fire parameters, the effect of increasing ambient wind velocity is to decrease the probability of interaction of particles with the plume and consequently decrease the "shadowing" effect of the plume. For a high-intensity fire over a large area, an increase in ambient wind speed from 5 mph to 10 mph reduces the area that receives no fallout. In addition, the assumption of a uniform ambient wind speed with altitude is generally not a valid one since the wind speeds usually increase with altitude. The "shadowing" effect of the plume is therefore expected to be less than that calculated for a uniform wind speed; the major difference is in the decrease in extent and width of the "shadow" for the upper portions of the plume.

The conclusions resulting from the study are intimately related to the assumptions which have lead to interaction cross section estimates of plumes. Several of these are based upon reported observations of fire behavior and if the latter are generally true, the assumptions could be considered reasonably well founded. It is desirable, however, for experimental studies to be carried out to verify or modify the specific model of fire fallout interaction presented here. Studies designed to provide cross section measurements of particle interactions as functions of ambient wind velocity, fire parameters, and particle size would be particularly useful in this regard. Laboratory studies would be recommended if simulation limitations such as fire intensity or gas generation rates, as pointed out by Broido and McMasters[4] and Corcos[21], could be eliminated. An experiment of the type

outlined by Lane and Lee[22] that proposes the dropping of tagged radioactive particles to the windward side of a full-scale fire plume and the subsequent measurement of surface density of particles at many locations could undoubtedly provide some experimental data that would be useful in testing and validating model parameters if simulation difficulties for smaller scale experiments cannot be overcome.

LINE FIRES

General Theory

Consider a line fire to consist of a uniformly heated surface of width x_0 and infinite in length along y perpendicular to x_0. Consider also that the heated and entrained gases expand only in the x and z (upward) directions. The bouyant gases should then form a column as viewed along the y axis, whose width increases with height.

For a section of the fire near the surface of length y_0 (a finite portion of y), the weight of heated gas, m_0, contained within a finite volume is given by

$$m_0 = \rho_0 x_0 y_0 \Delta z_o \tag{33}$$

where ρ_0 is the density of the heated gas in the volume near the earth's surface (assumed to be constant for all Z),

x_0 is the width of the fire at the surface,

y_0 is the length of the line fire under consideration, and

Δz_0 is an increment in height near the earth's surface.

Assume that over the altitude increment Δz_0 the upward velocity of the column is uniform. Under this assumption, the weight of Equation 33 may be written as

$$m_0 = \rho_0 x_0 y_0 \dot{z}_0 \Delta t \tag{34}$$

where $\dot{z}_0 \Delta t$ is equal to the distance Δz_0, z_0 is the initial vertical velocity, and Δt is the time interval over which $1/2 m_0 z_0^2$ Btu's of energy are transferred to the weight of air, m_0. An arbitrary distance, z, above the surface may be represented by

$$z = nx_0 \tag{35}$$

where n represents the number of units of x_0 for a given height, z, above the earth's surface. At some position above the surface, the change in gas volume during the time interval, Δt, corresponding to its expansion and/or increase in number of gas molecules as reflected in an increase in thickness, Δz, and an increase in spread across the width of the fire, Δx, is represented by

$$\Delta V = \left(x_0 + \Delta x\right) y_0 \Delta z \tag{36}$$

If a constant (or average) vertical velocity in the interval, Δz, is assumed, Equation 36 may be rewritten as

$$\Delta V = \left(x_0 + \Delta x\right) y_0 \dot{z} \Delta t \tag{37}$$

If Δx is assumed to be proportional to z (i.e., ratio of horizontal expansion to height of rise of the gas volume is constant), then Equation 37 becomes

$$\Delta V = \left(x_0 + 2\alpha z\right) y_0 \dot{z} \Delta t \tag{38}$$

in which α is the tangent of the angle of spread of the gases from the vertical in the x direction. Finally, if it is assumed that the mass contained in the volume ΔV is made up of gases corresponding to the original volume at its original density plus gases added from ambient air at ambient density, then the weight of gases contained in ΔV is given by

$$m = \rho_\infty \left(\Delta V - x_0 y_0 \dot{z}_0 \Delta t\right) + \rho_0 x_0 y_0 \dot{z}_0 \Delta t \tag{39}$$

in which ρ_∞ is the ambient gas density; upon substituting Equations 35 and 38, and differentiating Equation 35 with respect to time, Equation 39 becomes

$$m = \rho_0 x_0^2 y_0 \dot{n}_0 \Delta t \left\{ \frac{\rho_\infty n}{\rho_0 \dot{n}_0} + \frac{2\rho_\infty \alpha}{\rho_0 \dot{n}_0} n \dot{n} - \frac{\rho_\infty}{\rho_0} + 1 \right\} \tag{40}$$

where n_0 is the number of units of x_0 associated with $\dot{z}_0$ (z=0) and where the respective time differentials follow in order. Since $\rho_0 x_0^2 y_0 \dot{n}_0 \Delta t$ is equal to m_0, Equation 40 may be rewritten as

$$m = m_0 \left\{ \frac{\rho_\infty}{\rho_0 \dot{n}_0} + \frac{2\rho_\infty \alpha}{\rho_0 \dot{n}_0} n \dot{n} - \frac{\rho_\infty}{\rho_0} + 1 \right\} \tag{41}$$

The momentum of the gases at the altitude z is given by

$$\dot{mz} = m_0 x_0 \left[\frac{\rho_\infty}{\rho_0 \dot{n}_0} \dot{n} + \frac{2\rho_\infty \alpha}{\rho_0 \dot{n}_0} \dot{n}\, n - \frac{\rho_\infty}{\rho_0} + 1 \right] \dot{n} \tag{42}$$

and application of the law of conservation of momentum gives

$$\ddot{n} \left\{ 2\, n\, \dot{n} + \frac{1}{\alpha} n - \frac{\rho_0 \dot{n}_0}{2\rho_\infty \alpha} \left(\frac{\rho_\infty - \rho_0}{\rho_0} \right) \right\} + \dot{n}^3 = 0 \tag{43}$$

Substituting a parameter u as

$$u = n^2 - \frac{\rho_0 \dot{n}_0}{2\rho_\infty \alpha} \left(\frac{\rho_\infty - \rho_0}{\rho_0} \right) t \tag{44}$$

gives, upon sequential differentiation,

$$\dot{u} = 2\, n\, \dot{n} - \frac{\rho_0 \dot{n}_0}{2\rho_\infty \alpha} \left(\frac{\rho_\infty - \rho_0}{\rho_0} \right) \tag{45}$$

and

$$\ddot{u} = 2\, \dot{n}^2 + 2\, n\, \ddot{n} \tag{46}$$

Substitution of Equation 46 into Equation 43 gives

$$\ddot{n} \left(\dot{u} + \frac{1}{\alpha} \dot{n} \right) + \frac{1}{2} \ddot{u}\, \dot{n} - n\, \dot{n}\, \ddot{n} = 0 \tag{47}$$

Dividing through by $\dot{n}\,\ddot{n}$, the relation

$$\frac{d^2u}{dn^2} + \frac{2du}{dn} = 2\left(n - \frac{1}{\alpha}\right); \quad |\dot{n}\,\ddot{n}| > 0 \tag{48}$$

is obtained. The general solution of Equation 45 is

$$u = c_1 + \frac{\left(n - \frac{1}{\alpha}\right)^2}{2} - \frac{\left(n - \frac{1}{\alpha}\right)}{2} + c_2\, e^{-2n} \tag{49}$$

Replacing u by Equation 44 and differentiating with respect to time yields

$$\dot{n} = \frac{\dot{n}_0\left(\rho_\infty - \rho_0\right)}{2\alpha\rho_\infty\left[2c_2\, e^{-2n} + n + \frac{1}{\alpha} + \frac{1}{2}\right]} \tag{50}$$

The boundary conditions for Equation 50 are that $n = 0$ and $\dot{z}_0 = \dot{n}_0 x_0$ at $z = 0$, so that

$$c_2 = -\frac{\rho_0 + (1 + \alpha)\,\rho_\infty}{4\alpha\rho_\infty} \tag{51}$$

The vertical velocity along z is then given by

$$\dot{z} = \frac{\left(\frac{\dot{z}_0}{2\alpha}\right)\left(\frac{\rho_\infty - \rho_o}{\rho_\infty}\right)}{\left[\frac{z}{x_0} + \frac{1}{\alpha} + \frac{1}{2} - \left\{\frac{\rho_o + (1 + \alpha)\,\rho_\infty}{2\alpha\rho_\infty}\right\} e^{-\frac{2z}{x_0}}\right]} \tag{52}$$

Equation 52 indicates that the vertical velocity decreases rapidly with height during the period of early ascent of the heated air. At a height equal to several fire widths, however, the rate of rise becomes approximately proportional to the inverse of the height.

Butler[23] has suggested that maximum gas temperature resulting from wood fires is approximately the same from fire to fire. He estimates this temperature at about 2300°F. The results calculated by Nielsen, et al.[9] suggest the same behavior, although their maximum temperature is relatively constant near 3200°F. Assuming that the energy given to the plume may be estimated from gas expansion alone, a value for the initial gas density may be made from

$$\frac{\rho_\infty}{\rho_0} = \frac{T_0}{T_\infty} \tag{53}$$

where T_∞ represents the ambient gas temperature to the initial gas temperature. Estimating the initial gas density from Butler's experimentally based values of T_0 at about 1530°K and a T_∞ value of 300°K gives a value of 0.196 for ρ_0/ρ_∞ and a value of 0.804 for $(\rho_\infty-\rho_0)/\rho_\infty$.

The initial energy absorbed by the mass m_0 may be represented by

$$\frac{1}{2} m_0 \dot{z}_0^2 = 0.85 \; F \; x_0 y_0 k \Delta t \tag{54}$$

where k represents the energy released from burning wood; the numerical coefficient 0.85 is used to account for energy losses of about 15 percent due to radiation[24] for z_0 in ft/sec, k in Btu/lb, x_0 and y_0 in ft, and Δt in seconds.

Substitution of Equation 34 for m_0 in Equation 54 gives

$$\frac{1}{2} \rho_0 x_0 y_0 \dot{z}_0^3 \Delta t = 0.85 \; F \; x_0 y_0 k \Delta t \tag{55}$$

or

$$\frac{1}{2} \rho_0 \dot{z}_0^3 = 0.85 \text{ F k.} \tag{56}$$

Using the estimate of ρ_0 obtained from Equation 53, Equation 56 becomes

$$\dot{z}_0 = 68.17 \text{ F}^{1/3} \tag{57}$$

where k is assumed to be 2850 Btu/lb^2. Assuming α to have a value of 0.18, the vertical velocities for the line fires conforming to the model described here, after substitution of the above parameter values in Equation 52, are

$$\dot{z} \simeq \frac{152 \text{ F}^{1/3}}{\left[\frac{z}{x_0} + 6.06 - 3.83 \text{ e}^{-2 \frac{z}{x_0}}\right]} \tag{58}$$

The dependence of the vertical velocity on the fire width, x_0, as calculated from Equation 58, is given in Table 5. For the same fuel gas generation rates, the calculations show that the fire width produces increasingly high vertical velocities with height. To estimate the vertical velocities which might be produced were U.S. cities to suffer from line fires, use was made of building densities estimated for the City of Detroit. For surveys conducted in the city that included residential, business, and industrial sectors, the density of combustibles was estimated to range from 5.6 to 222.1 lb/ft^2 of wood or wood equivalent.[25] It may be estimated by linearly extrapolating Countryman's results from wood fires[14] to zero burn rate that 0.245 of the total available combustible material can be consumed during a 5-minute period of maximum fire activity. Using the densities of combustibles in the Detroit area as representative of northern U.S. cities, peak average (i.e., 0.245 of total combustibles consumed in 5 minutes of burn time) gas generation rates could range from 2.84×10^{-3} lbs/ft^{2}sec to 1.13×10^{-1} lbs/ft^{2}sec. Initial vertical velocities

Table 6

VARIATION OF VERTICAL VELOCITY WITH ALTITUDE

FOR $\dot{z}_0/F^{1/3}$ EQUAL TO 68.17

	x_0 (ft)								
Altitude (ft)	10	100	200	300	400	500	1,000	2,000	3,000
0	68.5	68.5	68.5	68.5	68.5	68.5	68.5	68.5	68.5
100	9.5	23.2	29.6	34.2	38.2	41.1	50.3	57.4	60.6
200	5.9	19.0	23.2	26.6	29.6	32.0	41.1	50.3	54.7
300	4.2	16.8	20.6	23.2	25.4	27.6	35.7	45.1	50.3
400	3.3	15.1	19.0	21.3	23.2	24.9	32.0	41.1	46.6
500	2.7	13.7	17.7	20.0	21.7	23.2	29.6	38.2	43.6
1,000	1.4	9.5	13.7	16.2	17.8	19.0	23.2	29.6	34.2
2,000	0.74	5.9	9.5	12.0	13.7	15.1	19.0	23.2	26.6
3,000	0.49	4.2	7.2	9.5	11.2	12.6	16.8	20.6	23.2

corresponding to these gas generation rates are 9.7 and 33.0 ft/sec. The maximum gas generation rate considered by Nielsen and coworkers[9] in their study of the convection column was 0.084 lb/ft^2 sec. The variation of velocity with height and fire width for this gas generation rate are presented in Table 6.

Where a uniform horizontal wind exists that (as expected) is normal to the length of the line fire, the leeward boundary of the rising plume may be found through evaluation of c_1 in Equation 49 for the boundary conditions that n = 0 and t = 0 and those leading to the value of c_2 given by Equation 51; the derived value of c_1 is then given by

$$c_1 = \frac{1}{2}\left[\frac{\rho_o + (1+\alpha)\rho_\infty}{2\alpha\rho_\infty}\right] - \frac{1}{2\alpha^2} - \frac{1}{2\alpha} \qquad (59)$$

With Equations 59 and 44, the time for the gas mass to rise to the height, z, is given by

$$t = \frac{\rho_\infty \rho_0 \alpha x_0}{\rho_0 \dot{z}_0 (\rho_\infty - \rho_0)} \left\{ \frac{z^2}{x_0^2} - \frac{z}{x_0}\left(1 + \frac{2}{\alpha}\right) - \left[\frac{\rho_0 + (1+\alpha)\rho_\infty}{2\alpha\rho_\infty}\right]\left[1 - e^{-2z/x_0}\right]\right\} \qquad (60)$$

The downwind boundary of the plume at the height, z, and time, t, is then given by

$$x_b = x_0 + \dot{x}_0 t \qquad (61)$$

where $\dot{x}_0$ is equal to the ambient wind speed. The value of $\dot{x}_b$ may be calculated directly by setting $(x_b/x_0)/\dot{x}_0$ equal to the right-hand side of Equation 60.

Curves showing the bending of the downwind boundary of gas plumes from line fires when subjected to constant ambient winds are given in Figures 20, 21, 22, and 23. Because the vertical velocities increase with increasing fire widths, less bending occurs for fires with the larger fire widths.

Table 7

VERTICAL VELOCITY WITH ALTITUDE (MPH)

$F = 0.084$ lbs/ft^{2}sec

	x_0(ft)								
Altitude (ft)	10	100	200	300	400	500	1,000	2,000	3,000
0	20.4	20.4	20.4	20.4	20.4	20.4	20.4	20.4	20.4
100	2.8	6.9	8.8	10.2	11.4	12.2	14.9	17.1	18.0
200	1.8	5.6	6.9	7.9	8.8	9.5	12.2	14.9	16.3
300	1.2	5.0	6.1	6.9	7.5	8.2	10.6	13.4	14.9
400	1.0	4.5	5.6	6.3	6.9	7.4	9.5	12.2	13.8
500	0.80	4.1	5.3	5.9	6.4	6.9	8.8	11.4	13.0
1,000	0.42	2.8	4.1	4.8	5.3	5.6	6.9	8.8	10.2
2,000	0.22	1.8	2.8	3.6	4.1	4.5	5.6	6.9	7.9
3,000	0.15	1.2	2.1	2.8	3.3	3.7	5.0	6.1	6.9

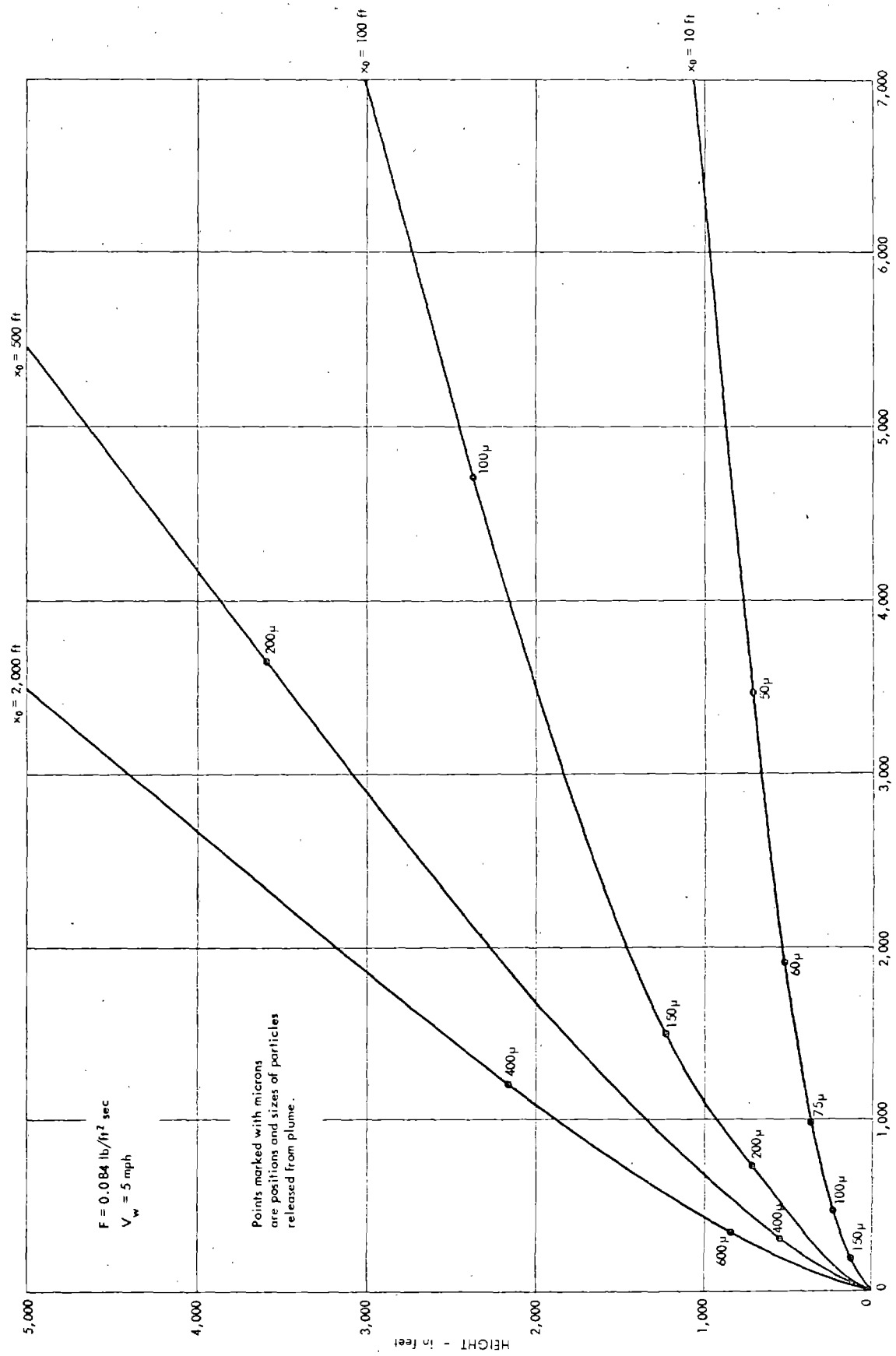

Fig. 20. Variation of Downwind Edge of Plume with Height Above the Line Fire Source

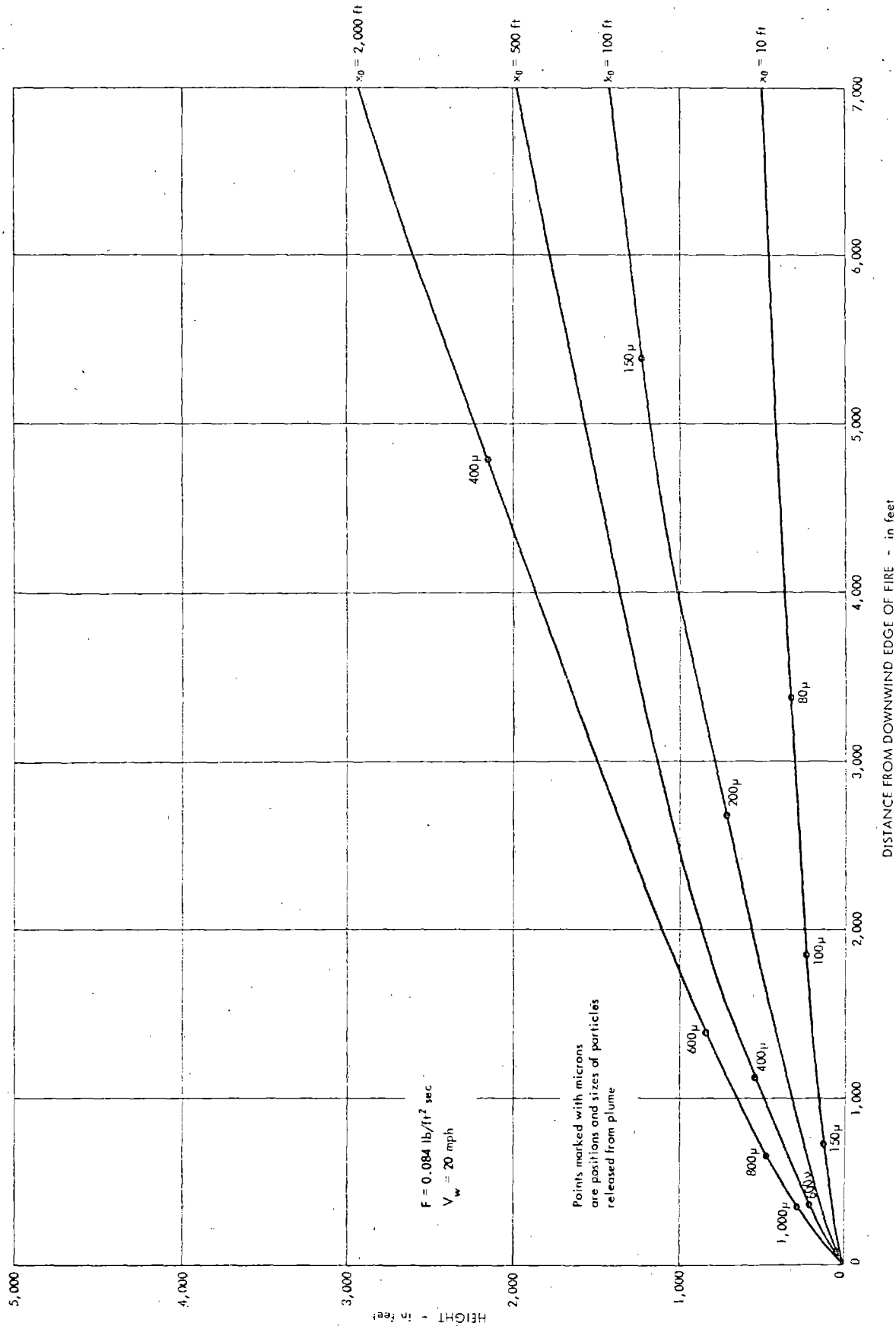

Fig. 21. Variation of Downwind Edge of Plume with Height Above the Line Fire Source

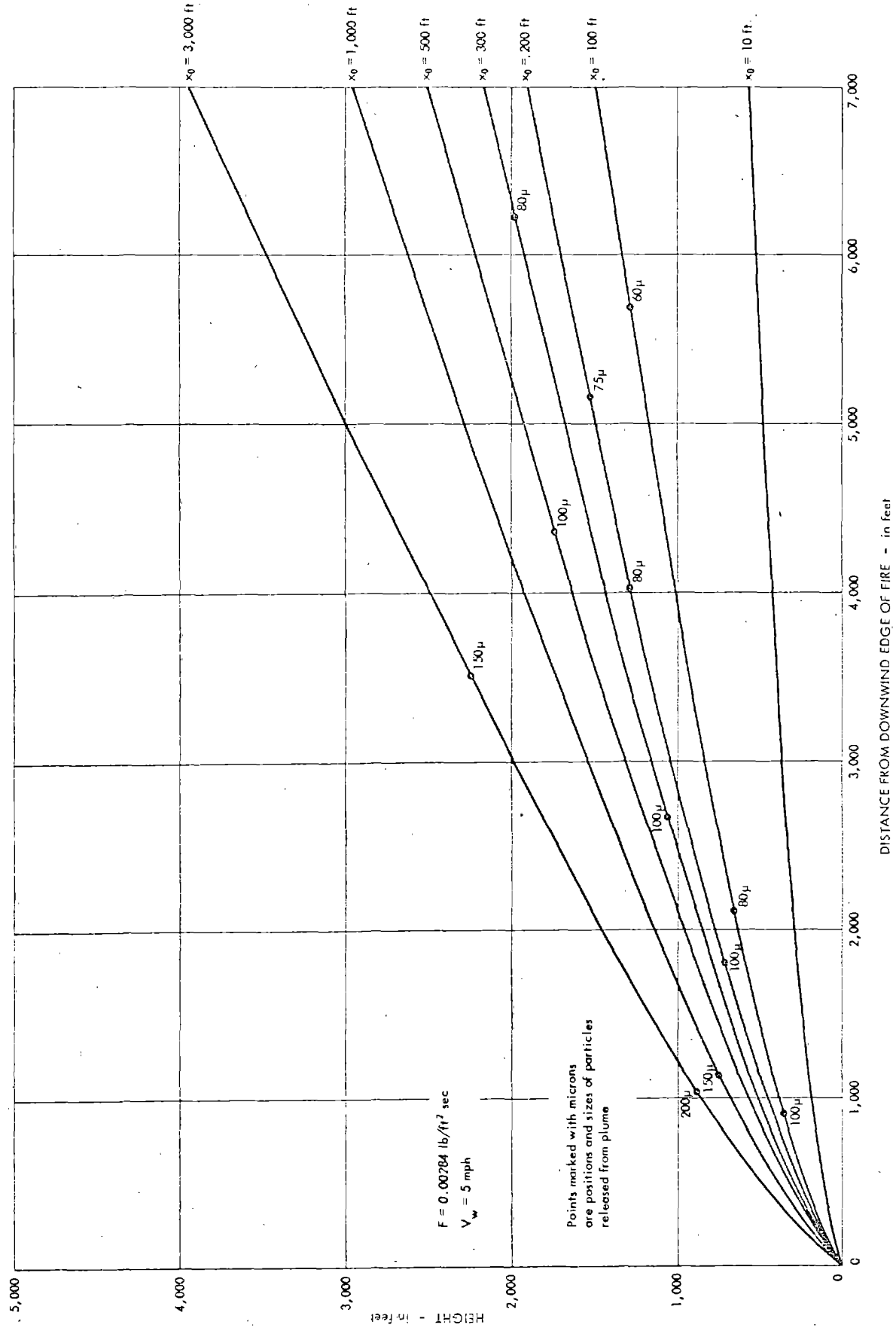

Fig. 22. Variation of Downwind Edge of Plume with Height Above the Line Fire Source

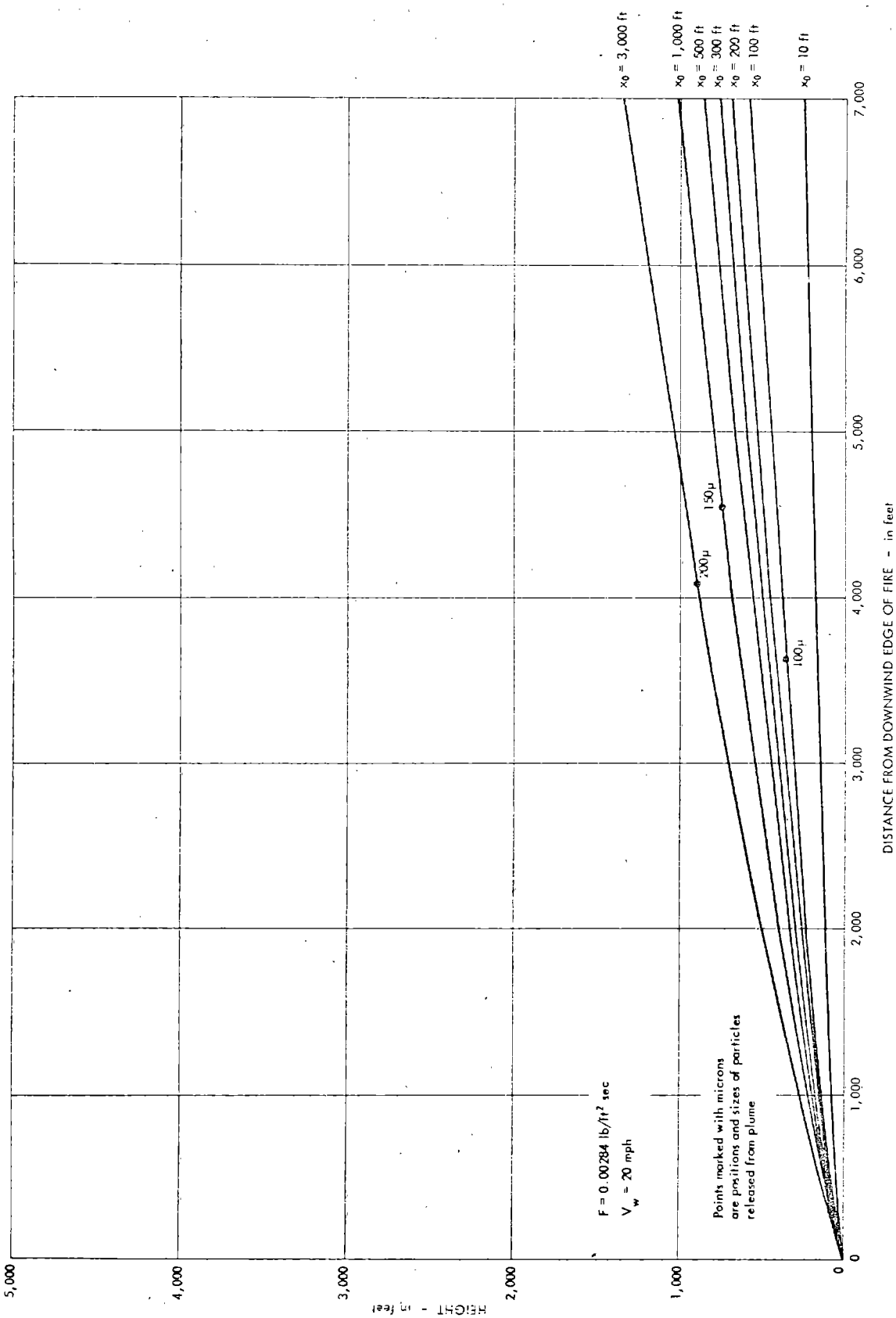

Fig. 23. Variation of Downwind Edge of Plume with Height Above the Line Fire Source

The heights at which particles that have penetrated the plume leave the downwind boundary were calculated by solving Equation 52 for the height z under the condition

$$v_z + \dot{z} = 0 \qquad (62)$$

where v_z is the "terminal" velocity of a spherical particle of density 2.5 and given radius. Heights at which particles fall out from plumes generated by a variety of fire conditions are shown in Figures 20 through 23. Even under the high gas generation rate used, particles of 400 μ diameter and greater do not achieve high altitude except with great fire widths. Small particles are carried with the plume, however, for great distances. It is expected that as the column of hot gases moves beyond the fire area, mechanisms other than those proposed here exist by which the plume is diluted and diffused.

In a situation where the line fire is burning when the fallout particles arrive, the particles which are intercepted by the upwind edge of the plume will, where $\dot{z}$ is greater than v_z, immediately begin to rise. The particles will continue to rise until the condition of Equation 62 is satisfied, at which time and height the particles will drift toward the downwind edge of the plume (at constant F and $\dot{x}_0$) and then fall back towards the earth, moving horizontally downwind with the ambient wind speed. Under ideal conditions, particles of a given diameter would be concentrated over the distance from the upwind edge of the fire to the downwind distance at which they began to fall back to earth (like water over a dam) and would form a line source of particles on the ground.

Under real conditions a line source would not occur because of fluctuations in wind speed, fire location change, and fire intensity, and because of the fact that the intercepted fallout particles would have a range in size or diameter. In the following illustrative calculation (Table 7) only the spread of the latter is taken into account for spreading the intercepted particles over a strip downwind but parallel to the line of an assumed fire. The computations for the effect of a line fire on the fallout pattern from a 1-MT yield

surface detonation are summarized in Table 7 for local wind speeds of 5 and 20 mph (although effective wind speed for the fallout deposition process is assumed to be 25 mph). The calculated downwind distance for a midrange particle diameter of 150 microns is 75 miles. The total width of area calculated to receive no fallout and for which no fire is in process at the time is given by $(X'-X_0-x_0)$. It is assumed that F, X_0 and x_0 remain constant during the whole fallout period. The width of the strip that is calculated to receive the redistributed fallout is given by $(X''-X')$. The results of Table 7 show that the width of both strips increases with ambient wind speed; for the larger fire (x_0 = 3,000 ft), the width of the no-fallout area is about 1.4 miles for U_0 = 5 mph and about 5.7 for U_0 = 20 mph. The overall trend in the variations of the width of the no-fallout area is thus 0.28 miles per mph increase in wind speed. For the fire, the width of the strip receiving an enhanced fallout deposition is 0.21 miles for U_0 = 5 mph and 0.84 miles for U_0 = 20 mph; the relative increase in area with wind speed of this strip is 0.042 miles per mph increase in wind speed. The width of both areas is approximately proportional to x_0 so that fire width and wind speed are both important factors in the effect of the line fire on the fallout deposition.

The values of $I_c = I_c^o + \Delta I_c$ are not very sensitive to the value of x_0 and decrease only slightly (25%) for an increase in ambient wind speed from 5 to 20 mph. The I_c values given in Table 7 may be low for the distance X' and high for the distance X'' because the total activity carried by the recycled particles was assumed to be spread evenly over the strip.

The results of Table 7 would be applicable to other locations in the crosswind direction if the line of the fire is approximately perpendicular to the centerline of the fallout (as is assumed for the calculations in Table 7). In such a case the distance variables remain the same and the I_s or I_c values decrease with distance from the centerline (all in the same relative amount).

Table 8

SUMMARY OF COMPUTATIONS FOR EFFECT OF A LINE FIRE ON DEPOSITION OF FALLOUT*

1. U_0 = 5 mph					
x_0(ft)	3,000	1,000	500	300	200
Δx(ft)	3,520	1,140	543	305	186
z(ft)	2,280	740	353	198	121
$\Delta t_f U_0$(mi)	0.865	0.283	0.135	0.076	0.046
X(mi)	77.100	75.688	75.333	75.191	75.119
X'(mi)	76.995	75.654	75.317	75.182	75.113
X'-X_0(mi)	1.995	0.654	0.317	0.182	0.113
X''(mi)	77.206	75.723	75.349	75.200	75.125
X''-X'(mi)	0.211	0.069	0.032	0.018	0.012
I_c^o(X')	257	269	272	274	274
I_c^o(X'')	255	267	272	274	274
ΔI_c	2,600	2,610	2,730	2,780	2,590
I_c(X')	2,857	2,879	3,002	3,054	2,864
I_c(X'')	2,855	2,877	3,002	3,054	2,864
2. U_0 = 20 mph					
x_0(ft)	3,000	1,000	500	300	200
Δx(ft)	14,070	4,550	2,170	1,220	744
z(ft)	2,280	740	353	198	121
$\Delta t_f U_0$(mi)	3.460	1.132	0.540	0.302	0.185
X(mi)	86.693	77.183	76.046	75.590	75.364
X'(mi)	81.272	77.045	75.980	75.553	75.341
X'-X_0(mi)	6.272	2.045	0.980	0.553	0.341
X''(mi)	82.115	77.321	76.112	75.627	75.387
X''-X'(mi)	0.843	0.277	0.132	0.074	0.046
I_c^o(X')	221	257	266	270	272
I_c^o(X'')	215	254	265	269	272
ΔI_c	2,050	2,030	2,040	2,060	2,040
I_c(X')	2,271	2,287	2,306	2,330	2,312
I_c(X'')	2,265	2,284	2,305	2,329	2,312

* W = 1.0 Mt; B = 50% fission; effective wind speed = 25 mph; fire at X_0 = 75.00 mi, Y_0 = 0.00 mi; $\bar{d}$ = 150 microns (V_f = 3.293 mph); V_f(max) = 3.745 mph; V_f(min) = 2.936 mph; $I_c^o(X_0)$ = 275 R/hr at 1 hr; I_c, I_c^o and ΔI_c values in R/hr at 1 hr; I_c = 0 for X = X_0 to X = X'; F = 0.00284 lb/sq ft-sec.

Although the no-fallout area downwind from the line fire is estimated to be much smaller than for the stationary large-scale fire, the fact that these fires apparently could, at the higher rates of burning, create narrow no-fallout strips should be of significance to the conduct of firefighting operations as well as to the movement of people during and after a combined fire and fallout operational situation.

Conclusions and Recommendations

Line fires can cause considerable alteration in fallout patterns. Generally, line fires create a zone immediately downwind from the fire virtually free from fallout and redistribute the intercepted fallout particles further downwind. The most significant interactions of fallout with line fires occur for high-intensity fires and for small and non-uniform intercepted particles. Under these circumstances, a substantial region immediately downwind from the fire is fallout free, while at some further distance downwind fallout deposition is increased markedly, due to the redistribution of particles in the fire updrafts.

As with the effects of plumes arising from fires of circular cross section and their interaction with fallout, it is desirable to experimentally verify the analytical results presented here. The interaction of line fires with fallout is conceptually simpler experimentally than for fires of circular surface cross section for laboratory studies. It is recommended that experimental studies be carried out on the laboratory scale.

REFERENCES

1. Schmidt, W., et al., Z. angew. Math. Mech., 21, 265, 351, 1941

2. Sutton, O. B., J. Met., 7, 307, 1960

3. Rouse, H., C. S. Yih, and H. W. Humphreys, Tellus, 4, 201, 1952

4. Broido, A., and A. W. McMasters, The Influence of Fire-Induced Convection Column on Radiological Fallout Patterns, California Forest and Range Experiment Station Forest Service, U.S. Department of Agriculture, Civil Defense Research Project, Series 2, Issue 13, Berkeley, California, 1959

5. Priestly, C.H.B., and F. K. Ball, Quart. J. Roy. Met. Soc., 81, 144, 1955

6. Morton, B. R., G. Taylor, and J. S. Turner, Proc. Roy. Soc., Series A, 234, 1, 1956

7. Murgai, M. P., and H. W. Emmons, J. Fluid Mech., 8, 611, 1960

8. Morton, B. R., Tenth Symposium (International) on Combustion, The Combustion Institute, Academic Press, 97, 3, 1965

9. Nielsen, H. J., L. Tao, and L. Wolf, Analysis of Convection Column Above a Fire Storm, IITRI Project A6004, Contract No. OCD-)S-62-82, Office of Civil Defense to IIT Research Institute, Chicago, 1963

10. Lommasson, T. E., and J. A. Keller, Fire Mortality Model, DC-TN-1056.1-1, The Dikewood Corporation, Albuquerque, New Mexico, 1966

11. Countryman, C. M., Mass Fires and Fire Behavior, U.S. Forest Service Research Paper PSW-19, Pacific Southwest Forest and Range Experiment Station, Berkeley, California, 1964

12. Countryman, C. M., Proceedings: Tripartite Technical Cooperation Program, Panel N-3 (Thermal Radiation) Mass Fire Research Symposium, DASA Information and Analysis Center, Santa Barbara, California, October 1967

13. Gaines, E. M., Proceedings: Tripartite Technical Cooperation Program, Panel N-3 (Thermal Radiation) Mass Fire Research Sumposium, DASA Information and Analysis Center, Santa Barbara, California, October 1967

14. Countryman, C. M., "Mass Fire Characteristics in Large-Scale Tests," Fire Technology, 1, No. 4, 1965

15. Sheppard, P. A., Sci. Prog., 37, 1949

16. Miller, C. F., "Distribution of Local Fallout," Chapter 3, Biological and Radiological Effects of Fallout from Nuclear Weapons, URS 702-1, OCD Contract N00228-68-C-2390, URS Research Company, Burlingame, California, May 1969

17. LaRiviere, P. D., and H. Lee, Postattack Recovery of Damaged Urban Areas, OCD Contract OCD-PS-64-201, Stanford Research Institute, Menlo Park, California, 1966

18. Glasstone, S., (ed), The Effects of Nuclear Weapons, Department of Defense, U.S. Government Printing Office, Washington, D.C., Revised Edition, 1964

19. Martin, S., R. Ramstad, and C. Colvin, Development and Application of an Interim Fire-Behavior Model, OCD Contract N00228-67-C-0710, URS Research Company, Burlingame, California, April 1968

20. Schubert, R., Examination of the Building Density and Fuel Loading in the Districts Eimsbüttel and Hammerbrook in the City of Hamburg as of July 1943, (Translation) OCD Contract N00228-67-C-1519, Stanford Research Institute, Menlo Park, California, 1969

21. Corcos, G. M., On the Small-Scale Non-Homogeneity of Fallout Deposition, Contract CD-SR-58-40, Office of Civil and Defense Mobilization, Series 2, Issue 2, Berkeley, California, 1958

22. Lane, William B., and Hong Lee, Effects of Mass Fires on Fallout Deposition, OCD Contract N00228-68-C-0158, Stanford Research Institute, Menlo Park, California, 1968

23. Butler, C. D., Operation FLAMBEAU - Civil Defense Experiment and Support, USNRDL-TR-68-143, U.S. Naval Radiological Defense Laboratory, San Francisco, California, 1968

24. Lee, S., and H. W. Emmons, J. of Fluid Mech., 11, 1961

25. Martin, Stanley B., Private Communication, URS Research Company, Burlingame, California, 1969

14. KEY WORDS	LINK A		LINK B		LINK C	
	ROLE	WT	ROLE	WT	ROLE	WT
FIRE						
FALLOUT						
LINE FIRE						
FIRE PLUME						
RADIAL VELOCITY						
FALLOUT PARTICLES						
FIRE RADIUS						

INTERACTION OF FALLOUT WITH FIRES (U)
URS 708-4
URS Research Company, San Mateo, California
September 1969 75 pp. Contract No. DAHC20-70-C-0214
Work Units 3124B and 3124C

UNCLASSIFIED

This report provides parametric relationships describing the possible interactions of fallout particles with air and gas currents arising from fires of circular area and from line fires. The effects that result from fallout – fire interactions due to varying fire dimensions and intensities, ambient wind velocities, fallout particle sizes, height of particle – fire plume interaction and other variables are given. Fallout field dislocations caused by fires are estimated for a number of fallout, fire, and ambient wind conditions relative to fields postulated to exist in the absence of fires. Under a number of fire input, meteorological, and fallout parameter values, the model output suggest that considerable alterations in fallout patterns could be produced.

INTERACTION OF FALLOUT WITH FIRES (U)
URS 708-4
URS Research Company, San Mateo, California
September 1969 75 pp. Contract No. DAHC20-70-C-0214
Work Units 3124B and 3124C

UNCLASSIFIED

This report provides parametric relationships describing the possible interactions of fallout particles with air and gas currents arising from fires of circular area and from line fires. The effects that result from fallout – fire interactions due to varying fire dimensions and intensities, ambient wind velocities, fallout particle sizes, height of particle – fire plume interaction and other variables are given. Fallout field dislocations caused by fires are estimated for a number of fallout, fire, and ambient wind conditions relative to fields postulated to exist in the absence of fires. Under a number of fire input, meteorological, and fallout parameter values, the model output suggest that considerable alterations in fallout patterns could be produced.

INTERACTION OF FALLOUT WITH FIRES (U)
URS 708-4
URS Research Company, San Mateo, California
September 1969 75 pp. Contract No. DAHC20-70-C-0214
Work Units 3124B and 3124C

UNCLASSIFIED

This report provides parametric relationships describing the possible interactions of fallout particles with air and gas currents arising from fires of circular area and from line fires. The effects that result from fallout – fire interactions due to varying fire dimensions and intensities, ambient wind velocities, fallout particle sizes, height of particle – fire plume interaction and other variables are given. Fallout field dislocations caused by fires are estimated for a number of fallout, fire, and ambient wind conditions relative to fields postulated to exist in the absence of fires. Under a number of fire input, meteorological, and fallout parameter values, the model output suggest that considerable alterations in fallout patterns could be produced.

INTERACTION OF FALLOUT WITH FIRES (U)
URS 708-1
URS Research Company, San Mateo, California
September 1969 75 pp. Contract No. DAHC20-70-C-0214
Work Units 3124B and 3124C

UNCLASSIFIED

This report provides parametric relationships describing the possible interactions of fallout particles with air and gas currents arising from fires of circular area and from line fires. The effects that result from fallout – fire interactions due to varying fire dimensions and intensities, ambient wind velocities, fallout particle sizes, height of particle – fire plume interaction and other variables are given. Fallout field dislocations caused by fires are estimated for a number of fallout, fire, and ambient wind conditions relative to fields postulated to exist in the absence of fires. Under a number of fire input, meteorological, and fallout parameter values, the model output suggest that considerable alterations in fallout patterns could be produced.